European Journal of Pharmaceutics and Biopharmaceutics 180 (2022) 33–47

Contents lists available at ScienceDirect

European Journal of Pharmaceutics and Biopharmaceutics

journal homepage: www.elsevier.com/locate/ejpb

Research paper

Pulmonary surfactant and drug delivery: Vehiculization of a tryptophan-tagged antimicrobial peptide over the air-liquid interfacial highway

Cristina García-Mouton [a], Elisa Parra-Ortiz [b], Martin Malmsten [b,c], Antonio Cruz [a], Jesús Pérez-Gil [a,*]

[a] Department of Biochemistry and Molecular Biology, Faculty of Biology, and Research Institute "Hospital 12 de Octubre (imas12)", Complutense University, 28040 Madrid, Spain
[b] Department of Pharmacy, University of Copenhagen, DK-2100 Copenhagen, Denmark
[c] Department of Physical Chemistry 1, University of Lund, SE-22100 Lund, Sweden

ARTICLE INFO

Keywords:
Air–liquid interface
Antimicrobial peptide
Drug delivery
Membrane
Pulmonary surfactant

ABSTRACT

This work evaluates interaction of pulmonary surfactant (PS) and antimicrobial peptides (AMPs) in order to investigate (i) if PS can be used to transport AMPs, and (ii) to what extent PS interferes with AMP function and vice versa. This, in turn, is motivated by a need to find new strategies to treat bacterial infections in the airways. Low respiratory tract infections (LRTIs) are a leading cause of illness and death worldwide that, together with the problem of multidrug-resistant (MDR) bacteria, bring to light the necessity of developing effective therapies that ensure high bioavailability of the drug at the site of infection and display a potent antimicrobial effect. Here, we propose the combination of AMPs with PS to improve their delivery, exemplified for the hydrophobically end-tagged AMP, GRR10W4 (GRRPRPRPRPWWWW-NH_2), with previously demonstrated potent antimicrobial activity against a broad spectrum of bacteria under various conditions. Experiments using model systems emulating the respiratory interface and an operating alveolus, based on surface balances and bubble surfactometry, served to demonstrate that a fluorescently labelled version of GRR10W4 (GRR10W4-F), was able to interact and insert into PS membranes without affecting its biophysical function. Therefore, vehiculization of the peptide along air–liquid interfaces was enabled, even for interfaces previously occupied by surfactants layers. Furthermore, breathing-like compression-expansion dynamics promoted the interfacial release of GRR10W4-F after its delivery, which could further allow the peptide to perform its antimicrobial function. PS/GRR10W4-F formulations displayed greater antimicrobial effects and reduced toxicity on cultured airway epithelial cells compared to that of the peptide alone. Taken together, these results open the door to the development of novel delivery strategies for AMPs in order to increase the bioavailability of these molecules at the infection site via inhaled therapies.

1. Introduction

The discovery of antibiotics is probably one of the most powerful achievements in the history of medicine. Since the discovery of penicillin by Alexander Fleming in 1928 [1], the number of deaths from infections has decreased enormously as a direct result of the development and use of antimicrobial compounds. However, the overuse and misuse of antibiotics over the years have led to the appearance of multidrug-resistant (MDR) bacteria, a public-health problem that causes hundreds of thousands of deaths in the world every year [2,3]. In an effort to solve this problem, antimicrobial peptides (AMPs), more recently known as host-defence peptides (HDPs), have attracted considerable attention as a potential solution. AMPs, which are present in essentially all external and internal interfaces, have been identified as an important part of the innate immune system in all living organisms, where they form a first line of defence against invading pathogens [4–6].

AMPs are small amphiphilic molecules that are ≈10-50 amino acids long with a net positive charge of generally + 2 to + 9 and a high proportion of hydrophobic residues (30–50 %). These features confer these peptides the capability to interact with and insert into negatively

* Corresponding author.
E-mail address: jperezgil@bio.ucm.es (J. Pérez-Gil).

https://doi.org/10.1016/j.ejpb.2022.09.018
Received 6 June 2022; Received in revised form 31 August 2022; Accepted 18 September 2022
Available online 23 September 2022

charged bacterial membranes, disrupting the permeability barrier imposed by the lipid membranes or inhibiting necessary biosynthetic processes [4,7,8]. AMPs not only act against a broad spectrum of bacteria, but also have antibiofilm function and play a role in wound healing and in the modulation of inflammatory responses to infection [2,9,10]. In spite of the numerous activities and efficacy demonstrated *in vitro* for many of the AMPs discovered in the last years, only 5 are currently approved for clinical use [5,11,12], so the efforts are now focused on trying to overcome the limitations in the use of these peptides in clinics.

One of the reasons why AMPs do not pass clinical trials is the low bioavailability at the site of infection, directly related to the delivery method. This is particularly challenging in the treatment of lower respiratory tract infections (LRTIs), a leading cause of death and disability [13–15], due to the highly stratified structure of the lung, together with the alveolar collapse derived from the infection. For delivery to the airways, pulmonary surfactant (PS) has previously been explored as a potential delivery system to overcome lung barriers (such as the branched structure of the respiratory system, fluid counterflows generated by ciliated cells, mucus, the proper PS and the presence of immune cells) and transport drugs to the distal airways [16–18]. PS is a lipid-protein material synthesized and secreted to the alveolar spaces by type II pneumocytes in order to reduce surface tension to a minimum, thereby avoiding alveolar collapse and minimizing the work of breathing. PS is mainly composed of lipids (around 90 % by mass) and an essential percentage (around 10 %) of four specific lung surfactant proteins: the hydrophilic collectins SP-A and SP-D, as well as the hydrophobic proteins SP-B and SP-C [16,19–21]. The main characteristic that makes PS attractive as a drug vehicle is its capability to incorporate hydrophobic drugs and to spread rapidly and efficiently over large air–liquid interfaces. This has previously been used to transport different types of drugs targeting the respiratory surface [22–26]. Based on this idea, we here propose the use of PS as a vehicle for AMPs in order to improve their interfacial-assisted delivery to the infection site in lung infections.

The combination of AMPs with PS as a delivery system has been proposed and evaluated in previous investigations [22,27,28]. To the best of our knowledge, however, no previous studies have addressed the use of peptides end-tagged with hydrophobic stretches, which can significantly enhance their incorporation into PS membranes competent to adsorb and spread through the interface while maintaining the antimicrobial functionality of the peptide. For this purpose, we used GRR10W4 (GRRPRPRPRPWWWW-NH_2), a peptide that has already demonstrated potent antimicrobial activity against both Gram positive (*Staphylococcus aureus; S. aureus*) and Gram negative (*Escherichia coli*; *E. coli* and *Pseudomonas aeruginosa; P. aeruginosa*) bacteria implicated in LRTI [29,30]. GRR10W4, derived from human proline arginine-rich and leucine-rich repeat protein (PRELP) and end-tagged with 4 tryptophan (W) residues, is short (15 residues), hydrophilic, highly charged (+5) and structurally disordered [29,30]. The interest in this peptide resides not only in its wide antimicrobial potency, but also in its pronounced selectivity for bacterial membranes, both at high and low ionic strength, together with sensitivity for the presence of cholesterol. The latter results in low toxicity against host cells, as previously demonstrated for erythrocytes and keratinocytes. It is also considerably resistant towards the action of both human and bacterial proteolytic enzymes [29–32]. Therefore, we hypothesized that the combination of GRR10W4 with an exogenous PS could be a strategy to increase the AMP bioavailability at the site of infection and improve the efficacy to treat lung infections.

The objective of this work was to determine whether the incorporation of the W-tagged GRR10W4 into surfactant membranes can significantly improve its transport along the air–water interface, while not detrimentally affecting the function of both entities. To do so, we employed a set of model systems and biophysical experimental setups to evaluate the interfacial activity of a fluorescently labelled GRR10W4 analogue, as well as the effect of the peptide on different PS biophysical properties such as surface activity, dynamics and lateral structure. Then, we studied the capability of PS to vehiculize the peptide interfacially and how it was released from the interface using the fluorescently labelled peptide. Finally, we determined whether the combination of both compounds affects the bactericidal activity of the AMP.

2. Materials and methods

Water was filtered and treated with a Merck-Millipore Direct-Q3 purification system and further distilled for the biophysical experiments.

2.1. Antimicrobial peptides

The peptides GRRPRPRPRP-NH_2, named GRR10, and GRRPRPRPRPWWWW-NH_2, named GRR10W4, were synthesized by the Peptide Synthesis Facility at Universitat Pompeu Fabra (Barcelona, Spain). To facilitate the detection of the AMP GRR10W4 in the fluorescence spectroscopy, epifluorescence microscopy and vehiculization experiments, a fluorescent derivative was used in the entire study. Thus, GRR10W4-Alexa488 (GRRPRPRPRPWWWWC-Alexa488-NH_2), from now on referred to as GRR10W4-F, was synthesized by Biopeptide Co. (San Diego, USA). The purity was > 95 %, as evidenced by HPLC. Peptides were used upon dilution to the required concentrations, therefore minimizing the concentration and the possible effects of any other reagent used during peptide synthesis and purification (i.e. trifluoroacetic acid).

2.2. Lipids

Synthetic phospholipids dipalmitoylphosphatidylcholine (DPPC; >99 %), palmitoyloleoylphosphatidylglycerol (POPG; >99 %), palmitoyloleoylphosphatidylcholine (POPC; >99 %) and cholesterol (>99 %), as well as the fluorescently labelled phospholipid Rhodamine-DOPE (Rho-DOPE; >99 %), were all purchased from Avanti Polar Lipids, Inc. (Alabaster, Alabama, USA).

2.3. Pulmonary surfactant preparations

Native pulmonary surfactant (NS) was isolated from bronchoalveolar lavages (BAL) of fresh slaughtered porcine lungs as previously described [33]. Briefly, BAL was filtered and centrifuged at 1,000 g for 5 min to eliminate cells and tissue debris. Then, it was ultracentrifuged for 1 h at 100,000 g and 4 °C to pellet surfactant complexes. The resultant pellets were resuspended in a 16 % NaBr 0.9 % NaCl solution and loaded into a discontinuous NaBr density gradient (ultracentrifuged at 120,000 g for 2 h at 4 °C), to purify the surfactant complexes from other cell membranes. NS complexes were re-suspended in 0.9 % NaCl solution and stored at − 80 °C until used. Then, the organic extract (OE) of these NS complexes, containing the lipids and the hydrophobic surfactant proteins, was obtained following the Blight and Dyer method [34]. The clinical pulmonary surfactant Poractant alfa, commercially available as Curosurf® (Csf), was obtained from Chiesi Farmaceutici S.p.A. (Parma, Italy). This is a porcine-derived surfactant prepared by reconstitution of an organic fraction of minced porcine lungs, containing polar lipids (with no cholesterol) and about 1 % of the hydrophobic surfactant proteins SP-B and SP-C. Surfactant and synthetic phospholipid concentrations were determined by phosphorus mineralization [35]. The mixture of surfactant proteins SP-B and SP-C was purified from the OE of minced porcine lungs by size exclusion chromatography in organic solvents using a Sephadex LH-20 column (GE Healthcare; Little Chalfont, UK), as previously described [36], in order to separate the mixture of both hydrophobic proteins from surfactant lipids.

To prepare multilamellar suspensions from OE or synthetic lipids, proper volumes of the materials according to each experiment were dried under a nitrogen stream and under vacuum for 2 h to remove organic solvent traces and forming a dry lipid film. The dried films were

reconstituted by hydration in buffer solution (Tris 5 mM, NaCl 150 mM, pH 7.4) incubating in Thermomixer for 1 h at 45 °C, a temperature above the melting temperature of the phospholipids, shaking at 1400 rpm every 10 min, obtaining multilamellar vesicle suspensions (MLV). When combined with the peptide, the appropriate volume of GRR10W4-F was added to the vesicles to have a proportion of 5 mass%, and further incubated for 30 min at 37 °C, to favour the interaction between both components.

2.4. Interfacial balances

Characterization of the interfacial activity of GRR10W4-F, its interaction with lipids and further vehiculization by surfactant was assessed using two surface balance-based setups: an adsorption Wilhelmy balance and a double-balance setup connected through the interface.

Interfacial adsorption of GRR10W4-F and interaction with lipids. To characterize the interfacial adsorption of GRR10W4-F, as well as its interaction with interfacial lipid films, a Wilhelmy trough (NIMA technologies, Coventry, UK) was used. This balance consists of a Teflon trough filled with 1.8 mL of a buffered solution (Tris 5 mM, NaCl 150 mM, pH 7.4), constantly stirred and thermostated at 25 °C, with a pressure sensor that allows monitoring changes in surface pressure over time. This balance only provides information about the adsorption and spreading of the material under static conditions, which is far from the situation in the *in vivo* scenario. However, this method is a simple and reproducible technique to obtain an essential information at the beginning of the study. In the adsorption experiments, after 1 min equilibration, different amounts of the peptide were injected into the subphase diluted in the same buffer to a final concentration ranging from 0.25 to 5 μM, and the changes in surface pressure were monitored for 25 min. In separate experiments, to evaluate the insertion of GRR10W4-F into interfacial phospholipid films, small volumes of the desired lipid solutions at 0.1 mg/mL in chloroform:methanol (2:1 v/v) were spread dropwise at the air–liquid interface to form lipid monolayers at different initial surface pressures (Π_i). To allow for full evaporation of the organic solvents, after 10 min the peptide was injected into the subphase of the balance at a final concentration of 1 μM and changes in surface pressure were monitored for 25 min. Experiments to study the effect on the adsorption capabilities of surfactant in combination with GRR10W4-F were also performed in the Wilhelmy balance. MLVs of different lipid and lipid-protein composition were formed as described before, mixed or not with 5 % (by mass with respect to the lipids) of the different peptide versions (i.e., GRR10, GRR10W4 or GRR10W4-F). Two μL of the MLVs at 1 mg/mL or 2 mg/mL, as convenient, were deposited onto the air–liquid interface, and changes in surface pressure were measured for further 15 min.

Interfacial vehiculization of GRR10W4-F by PS. In order to study the capability of PS to vehiculize GRR10W4-F through the air–liquid interface, we employed an *in vitro* double-balance setup designed and described by Hidalgo *et al.* [26]. This consists of the combination of a Wilhelmy trough (surface area of 10 cm^2) as a donor compartment, and a Langmuir-Blodgett balance (surface area of 60–184 cm^2; NIMA technologies, Coventry, UK) as a recipient compartment, both connected by an interfacial paper bridge (6 cm length × 1 cm width) made of hydrated filter paper (No. 1 Whatman filter paper, GE Healthcare Life Sciences). This setup is aimed to mimic a respiratory air–liquid interface with the delivery at the upper airways and the possible interfacial travel to the distal airways, and demonstrated to provide results on vehiculization that compare well with those found *in vivo* [26]. For these experiments, the aqueous subphase in each trough, continuously thermostated at 25 °C, was Tris 5 mM, NaCl 150 mM, pH 7.4. Five mass% GRR10W4-F was combined with different surfactant preparations as explained above and the resulting MLVs were deposited dropwise (15 μL, 50 mg/mL) onto the interface of the donor trough. Changes in surface pressure were monitored in both compartments and allowed to equilibrate during 30 min to let the material travel from the donor to the recipient compartment. Finally, the bridge was removed and the interface at the recipient trough was collected by aspiration until the surface pressure dropped to ~ 0 mN/m to further measure the fluorescence of interfacially transported GRR10W4-F. The flexible tube used for the aspiration was placed at the surface to aspirate just the interface in order to minimize the volume of subphase collected. The use of a Langmuir-Blodgett balance as the recipient compartment allowed to test the contribution to the vehiculization process of breathing-like compression-expansion cycles of the transferred interfacial material. In order to do this, the bridge was removed 30 min after sample injection in the donor trough, and the vehiculized film in the recipient compartment was subjected to 10 compression-expansion cycles (65 cm^2/min of barrier speed). The Langmuir-Blodgett balance also allowed transference of the interfacial film onto glass coverslips in order to observe its structure and lateral organization under an epifluorescence microscope, which was done at the end of each experiment.

2.5. Captive bubble surfactometer (CBS)

To evaluate if the incorporation of GRR10W4-F could compromise surfactant function, we investigated surfactant performance using a captive bubble surfactometer (CBS). As described by Ravera *et al.* [37], there are different methodologies to study the function and structure of surfactant, providing information about different aspects. CBS is, as the constrained drop surfactometer, one of the preferred methods to study the interfacial properties of PS under controlled and reproducible conditions, but the former is actually considered the most effective technique to study dynamic changes in surface tension under breathing-like conditions [38]. The CBS allows evaluation of the capability of PS to interfacially adsorb, re-spread and reduce the surface tension while being subjected to compression-expansion cycles under physiologically-relevant conditions. We used a modified version [39] of the device originally designed and described by Schürch *et al.* [40]. Briefly, this consists of a sealed glass chamber filled with a buffer solution (Tris 5 mM, NaCl 150 mM, 10 w/v % sucrose, pH 7.4) thermostated at 37 °C. In this chamber, a small air bubble (2 mm Ø) is created, and a piston modifies the hydrostatic pressure to compress and expand the bubble, emulating the breathing dynamics. The bubble is continuously monitored using a camera (Pulnix TM 7 CN; Sunnyvale, CA, USA), and the surface tension is calculated from the bubble dimensions based on Laplace's law [41]. Using a small capillary tube, ~300 nL of each sample at a lipid concentration of 15 mg/mL were injected near the air bubble interface. The initial adsorption of the material was monitored for the first 5 min. Subsequently, the chamber was sealed and the bubble was rapidly expanded (to ~ 25 % increase of its volume) to evaluate the re-spreading of the material over the interface while maintaining low surface tension values, during the so-called post-expansion adsorption. Four slow quasi-static cycles were performed after this, in which the film was compressed by stepwise area reductions (20 % in each step) to reach the minimal surface tension values before the film collapses. A delay of 1 min between these cycles allows the interfacial film to reorganize. Finally, the bubble was subjected to 20 quick dynamic cycles in 1 min to analyse the behaviour of the material under physiological-like dynamic conditions.

2.6. Fluorescence spectroscopy

The capability of PS to vehiculize GRR10W4-F was evaluated by measuring the fluorescence of the dye Alexa Fluor 488 ($\lambda_{excitation}$ = 490 nm, $\lambda_{emission}$ = 520 nm), using an Aminco Bowman Series 2 spectrofluorometer. The interface of the recipient compartment was carefully collected by aspiration of the surface until the surface pressure dropped to ~ 0 mN/m (~1 mL collected) and the emission spectra were recorded at 25 °C. For comparison, the volumes of all samples were equalled and measured at the same sensitivity. To correct for the actual quantum yield of GRR10W4-F fluorescence intensity in the different environments

provided by its combination with different surfactant preparations, 5 mass% GRR10W4-F was incorporated into NS, OE or Csf, and the fluorescence of AlexaFluor488 was measured in different dilutions of each sample under the same conditions. The values thus obtained were used to relativize the fluorescence at the plots comparing the different samples.

2.7. Epifluorescence microscopy

To analyse the interfacial structure of transferred PS interfacial films in the presence of GRR10W4-F resulting from the vehiculization experiments, OE was doped with 1 mol% Rho-DOPE and the surface film transferred onto glass coverslips under continuous compression (barrier speed: 25 cm^2/min; dipper speed: 5 mm/min) following the Langmuir-Blodgett COVASP method [42]. Transferred films were analysed under an epifluorescence microscope Leica DM 4000B (Leica Microsystems, Germany), using the filter cube L5 (excitation 440–520 nm; emission 497–557 nm) to image GRR10W4-F, and the filter cube TX2 (excitation range 520–600 nm; emission range 570–720 nm) to image OE-Rho-DOPE. Images were acquired with an ORCA R2 10,600 camera (Hamamatsu Photonics K.K.).

2.8. Antimicrobial assays

Escherichia coli (*E. coli*) DSM 1103 (ATCC 25922, DSMZ, Braunschweig, Germany) was selected for robustness and wide availability to test the antimicrobial effect of GRR10W4-F in combination with OE, even though this is not a respiratory pathogen, it is simpler to work with and is not likely to dramatically influence the physicochemical take home message of our study. Minimal inhibitory concentration (MIC) and viable count assay (VCA) were used to evaluate the capability of the peptide to inhibit bacterial growth and kill bacteria, respectively.

Minimal Inhibitory Concentration (MIC) determination. The minimal inhibitory concentration (MIC) for GRR10W4-F towards *E. coli* was determined following the microdilution method described in [43]. Briefly, three to five colonies obtained from an overnight agar plate were suspended into Mueller-Hinton (M−H) broth and growth to a turbidity of 0.5 units (~10^8 cfu/mL). Since the antimicrobial activity of AMPs can be affected by growth media components [44], the assay was performed in a buffer solution (Tris 10 mM, NaCl 150 mM, glucose 5 mM, pH 7.4). For this, adjusted bacteria were washed and diluted in buffer. Samples of AMP, OE, or OE combined with 5 mass% GRR10W4-F, were diluted in buffer at concentrations 2 times higher than that required in the test by serial dilution in a 96-well polypropylene plate. OE was used as PS preparation in order to avoid influence of any anti-bacterial effect of the hydrophilic surfactant proteins A and D present in full PS. Each sample solution was inoculated to the corresponding well, together with the bacterial suspension to obtain a final inoculum of 5x10^5 cfu/mL. The plate was incubated at 37 °C with humidity for 16–20 h. MIC was considered to be the lowest concentration at which the bacterial pellet was visibly affected or no growth was detected.

Viable Count Assay (VCA). Three to five overnight colonies of *E. coli* were grown in M−H broth to a concentration of ~ 10^8 cfu/mL. Bacteria were washed and diluted in buffer Tris 10 mM, NaCl 150 mM, glucose 5 mM, pH 7.4 to a concentration of 4x10^6 cfu/mL. AMP, OE or OE with 5 mass% GRR10W4-F were suspended in buffer to concentrations 2 times higher than that required in the test, and 25 μL of the different dilutions then incubated with 25 μL of bacteria (final inoculum of 2x10^6 cfu/mL) at 37 °C for 2 h. Finally, serial dilutions were plated on M−H agar, followed by incubation at 37 °C overnight, and cfu determination.

2.9. Cytotoxicity assay

A549 pulmonary cells (ATCC CCL-185) were grown in Dulbecco's modified Eagle medium (DMEM) supplemented with F12 nutrient mixture, 10 v/v % of heat-inactivated fetal bovine serum (FBS) and 50 units/mL of penicillin/streptomycin at 37 °C in 5 % CO_2 humid atmosphere. Cells were seeded in 96-well plates at a density of 7500 cells/well and allowed to settle overnight. A549 in DMEM-F12-penicillin/streptomycin without FBS were incubated overnight with 5, 10, 20 or 40 μM of GRR10W4-F alone or combined with OE (at 5 mass%), or with OE alone (2.23, 1.12, 0.56 and 0.28 mg/mL). After incubation, the wells were washed with PBS to remove excess surfactant, followed by addition of 100 μL fresh media plus 10 μL 4-[3-(4-Iodophenyl)-2-(4-nitro-phenyl)–2H-5-tetrazolio]-1,3-benzene sulfonate (WST-1; Sigma Aldrich, St. Louis, Missouri, USA) and incubation at 37 °C in 5 % CO_2 for 30 min. The tetrazolium salt WST-1 is reduced to a soluble formazan by cellular enzymes, so the amount of formazan produced correlates to the number of metabolically active cells. Finally, the absorbance at 450 nm was measured, and background absorbance measured at 630 nm was subtracted. Results are represented as mean and standard deviation values obtained from biological triplicates.

2.10. Statistical analysis

Data are expressed as mean and standard deviation. Results comparisons were conducted using One-Way ANOVA followed by Tukey post-hoc test, Two-Way ANOVA followed by Bonferroni post-hoc test or unpaired *t*-test when appropriate. A p-value below 0.05 was considered to be significant. Analyses were carried out using GraphPad Prism 7 (v. 7, GraphPad Software, San Diego, California, USA).

3. Results

3.1. Characterization of GRR10W4-F interfacial properties

The surface activity of GRR10W4-F was first characterized on air-buffer interfaces using a Wilhelmy balance (Fig. 1**A**). Different amounts of the peptide were injected into the subphase of a small Teflon trough, causing a rapid increase in surface pressure (Fig. 1**B-C**), meaning that GRR10W4-F is able to adsorb by itself and form a stable film at the air–liquid interface (see the Π-time isotherms of all the samples and replicas in the supplementary **Figure S1** available in https://doi.org/10.6084/m9.figshare.20747824). The surface behaviour of the peptide was dependent on its final concentration at the subphase, following an apparent hyperbolic ratio (Fig. 1**C**) (R^2 correlation value of 0.94). This leads by extrapolation to an estimated theoretical maximum surface pressure of 12.1 ± 1 mN/m at high peptide concentration.

We next evaluated the adsorption to interfaces previously occupied by phospholipids. For this, 1 μM was selected as an optimal peptide concentration to perform these experiments, as it produced a measurable increase in surface pressure (~3.5 mN/m) but far from surface saturation. Various lipid mixtures were chosen in order to evaluate different aspects of the interaction: DPPC, as a saturated phospholipid and the main surface-active phospholipid species in PS; POPG, as a representative anionic unsaturated phospholipid in PS; and the mixture DPPC:POPC:POPG:Chol (50:25:15:10 mass ratio), as a model to mimic PS lipid composition, including its saturated/unsaturated and zwitterionic/anionic phospholipid ratios and its cholesterol content. DPPC organizes in gel phase (L_β) with low rotational mobility and high packing, while POPG forms disordered liquid-crystalline phase (L_α) at the temperature tested. In the case of the lipid mixture, cholesterol generates a segregation of liquid-ordered (L_o) and liquid-disordered (L_d) phases. Fig. 2**A** shows that injection of GRR10W4-F into the subphase caused an increase in surface pressure in all the lipid monolayers assayed, indicating peptide insertion. By plotting the increase in surface pressure produced upon addition of the peptide versus the initial surface pressure values for each lipid monolayer, we could estimate the critical pressure of insertion (Π_c), obtained from the intersection of the linear regression with the x-axis. This is a theoretical value that represents the maximal initial pressure still allowing the insertion of the peptide into a given preformed lipid (mono)layer. As observed in the graphs, the highest

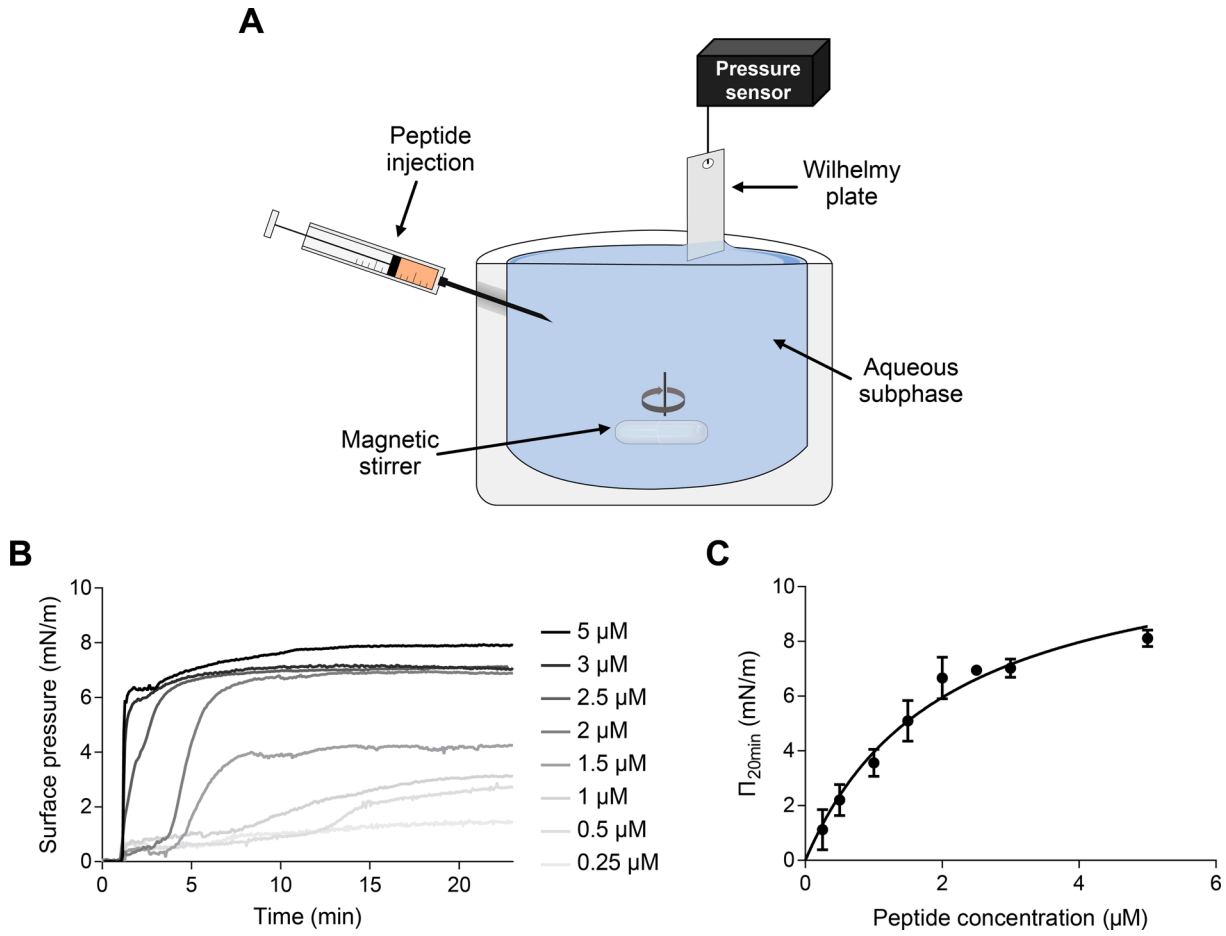

Fig. 1. Interfacial behaviour of GRR10W4-F. (A) Schematic representation of an interfacial adsorption experiment at the Wilhelmy balance. (B) Surface pressure (Π)-time isotherms of GRR10W4-F upon injection into the subphase of a Wilhelmy balance to reach final peptide concentrations of 0.25, 0.5, 1, 1.5, 2, 2.5, 3 and 5 μM. One representative replica of at least 3 is shown in the graph. (C) Maximum surface pressure achieved 20 min after injection of each peptide concentration. Data represent mean and standard deviation calculated from a minimum of 3 independent experiments. The solid line illustrates the hyperbolic best fit to the data ($r^2 = 0.94$).

increase in surface pressure occurred as a consequence of the insertion of the peptide into POPG monolayers. This indicates the critical establishment of electrostatic interactions between the net positive charge of GRR10W4-F and the anionic phospholipid. Also, likely, the lower cost of the insertion of the peptide into less packed monolayers such as those formed by the unsaturated phospholipid compared with the insertion in the other two systems. Π_c values are different for the insertion of the peptide into the three tested monolayers, being 19.3 ± 0.5 mN/m for DPPC monolayers, 32.2 ± 0.5 mN/m for POPG monolayers, and 27.5 ± 0.9 mN/m for the insertion into DPPC:POPC:POPG:Chol films. The peptide presents the ability to interact and insert into phospholipid membranes with different composition and lateral packing in the order of 30 mN/m, although inserting preferentially into less packed anionic monolayers.

After confirming the interaction of GRR10W4-F with lipid monolayers, we studied the effect of this interaction on the adsorption capabilities of pulmonary surfactant-like vesicles pre-mixed with the AMP, specifically those containing cholesterol and/or hydrophobic surfactant proteins. For this, we reconstituted MLVs with different lipid and lipid-protein mixtures that emulate PS composition: 1) DPPC:POPC:POPG (50:25:15 mass ratio); 2) DPPC:POPC:POPG + 2 % SP-B/SP-C mixture (total protein-to-lipid mass ratio); 3) DPPC:POPC:POPG:Chol (50:25:15:10 mass ratio); and 4) DPPC:POPC:POPG:Chol + 2 % SP-B/SP-C mixture (total protein-to-lipid mass ratio). Then, lipid or proteolipid MLVs were incubated with 5 mass% GRR10W4-F and their mutual surface activity was evaluated again using the Wilhelmy balance. The surface pressures achieved 10 min after injection into the interface are presented in Fig. 2**B**. The addition of the peptide alone at the concentration used only led to a slight increase in surface pressure (<10 mN/m). Similarly, the combination of the peptide with lipid MLVs did not produce any significant increase in the adsorption capabilities of purely lipidic vesicles. In contrast, we can observe that the presence of the hydrophobic surfactant proteins was essential to allow the efficient interfacial adsorption of the MLVs to very high surface pressures in the order of 20 mN/m. Strikingly, the addition of 5 mass% GRR10W4-F to these proteolipid MLVs produced a further significant increase in the surface pressure reached 10 min after the injection of the material, an effect that was only observed in the presence of SP-B and SP-C in the mixture. The presence of cholesterol in the lipid composition did not seem to affect the interfacial activity of the vesicles nor the effect of GRR10W4-F on their adsorption capabilities.

Finally, to determine whether the improved adsorption observed for the MLVs combined with GRR10W4-F was an effect of the attached Alexa488 or the tryptophan-tag, we performed similar experiments with the peptide without the Alexa fluorophore (GRR10W4) and without the hydrophobic tag (GRR10). We reconstituted MLVs of DPPC:POPC:POPG (50:25:15 mass ratio) + 2 % SP-B/SP-C that were incubated afterwards with 5 mass% of each AMP, as appropriate. Two μL of the sample at 1 mg/mL (phospholipid concentration) were injected at the interface and the surface pressure achieved 10 min after is represented in Fig. 2**C**. The three different variants of the AMP improved the adsorption of the MLVs. Furthermore, we could observe a progressive improvement in the

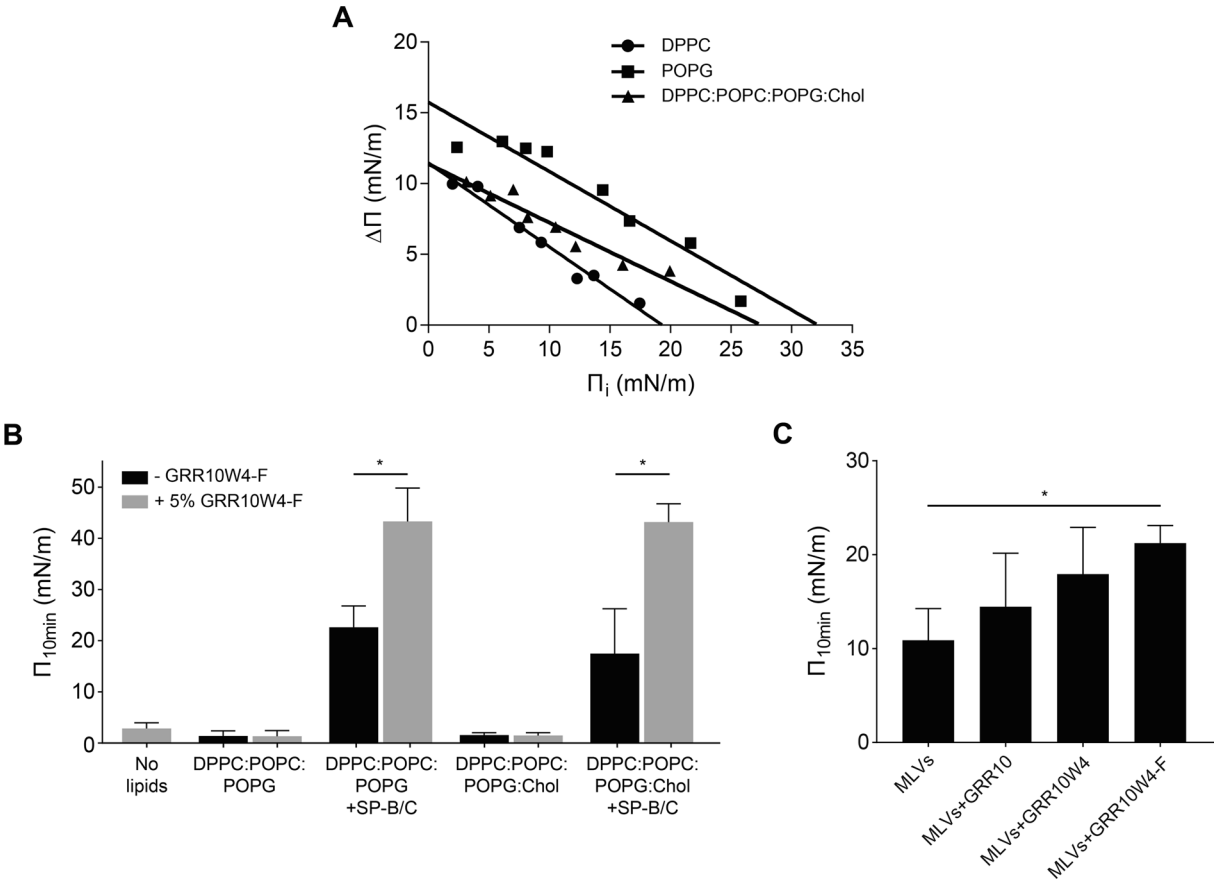

Fig. 2. Interaction of the antimicrobial peptide with lipid surfaces. (A) Increase in surface pressure (ΔΠ) registered 20 min after GRR10W4-F injection versus the initial surface pressure (Π_i) of DPPC, POPG or DPPC:POPC:POPG:Chol (50:25:15:10 w/w) monolayers. The lines represent the linear regression that best fits the experimental data (DPPC: $r^2 = 0.97$; POPG: $r^2 = 0.92$; DPPC:POPC:POPG:Chol: $r^2 = 0.93$). (B) Surface pressure achieved 10 min after the interfacial injection of 2 μL of MLVs (2 mg/mL) of different composition in the absence or in the presence of GRR10W4-F (5 mass%). Mean and standard deviation calculated from at least 3 replicates. Unpaired *t*-test (*) $p < 0.05$. (C) Surface pressure achieved 10 min after the interfacial injection of 2 μL of MLVs made of DPPC:POPC:POPG + 2 mass% SP-B/SP-C (1 mg/mL) in combination with 5 mass% of GRR10, GRR10W4 or GRR10W4-F. Mean and standard deviation calculated from at least 3 replicates. One-way ANOVA ($p = 0.026$) followed by Tukey post-hoc test: (*) $p < 0.05$ and > 0.01.

adsorption of the vesicles upon the incorporation of the tryptophan tag and the Alexa fluorophore, although statistical significance was observed only for GRR10W4-F, demonstrating the importance of large hydrophobic domain on the peptide for boosting this effect.

3.2. Impact of GRR10W4-F on pulmonary surfactant functional properties

Once the interfacial activity of the AMP and its interaction with lipid-coated surfaces and lipid or proteolipid vesicles were verified, we next analysed whether its incorporation into surfactant membranes would compromise the functional properties of PS in terms of interfacial spreading. To do so, we used the CBS setup to evaluate surfactant function in the presence of the AMP under physiologically-relevant conditions. In these experiments, we tested the effect of 5 mass% GRR10W4-F on proteolipid suspensions reconstituted from OE. Fig. 3 summarizes the isotherms obtained from CBS experiments carried out in the absence or presence of GRR10W4-F. As it had been previously observed in the Wilhelmy balance, the incorporation of GRR10W4-F into reconstituted OE membranes improved the interfacial adsorption properties of the material, which reduced the surface tension to equilibrium values (25.9 ± 1.4 mN/m) in just one second, while equilibrium surface tensions were reached in around 10–30 s for OE. A significant difference in the surface tension values between both materials could be observed already at 1 s ($p = 0.07$). Enhanced re-spreading capabilities were also observed during the post-expansion adsorption of OE containing the peptide, as the surface tension barely increased right after bubble expansion (only up to 28.3 ± 2.6 mN/m) and again quickly dropped to equilibrium values within the first seconds. This indicates extremely efficient re-spreading, in contrast with the behaviour of the OE control, which increased up to 38.6 ± 6.5 mN/m before reaching equilibrium values again. Therefore, the AMP clearly enhanced OE surface activity both in clean air–water interfaces and in expanded interfaces partially coated with proteolipid material. Furthermore, quasi-static compression-expansion cycles, consisting of stepwise 20 % area expansions that allow for material equilibration and reorganization for 4 s, show that incorporation of GRR10W4-F into OE membranes resulted in a shorter plateau during the first compression. The plateau is associated to the lateral reorganization and the formation of three-dimensional structures due to compression of the film, which is crucial to produce maximal packing and reach minimal surface tension. In addition, a lower area reduction (0.31 ± 0.04) was required to reduce the surface tension to minimal values (~1–2 mN/m) than in the absence of peptide (0.46 ± 0.09), suggesting a faster enrichment of the film in saturated lipids. After the first quasi-static cycle, the isotherms did not show any further hysteresis and the area compression was reduced. In the absence of peptide, and analogously to the slower kinetics found for the interfacial adsorption results discussed above, the compression needed to minimize the surface tension was substantially decreased over the cycles, so 4 quasi-static cycles were required to produce non-hysteretic isotherms. The rapid dynamic cycles performed afterwards, consisting of area changes of 25 % at a rate of 20 cycles/min, resulted in

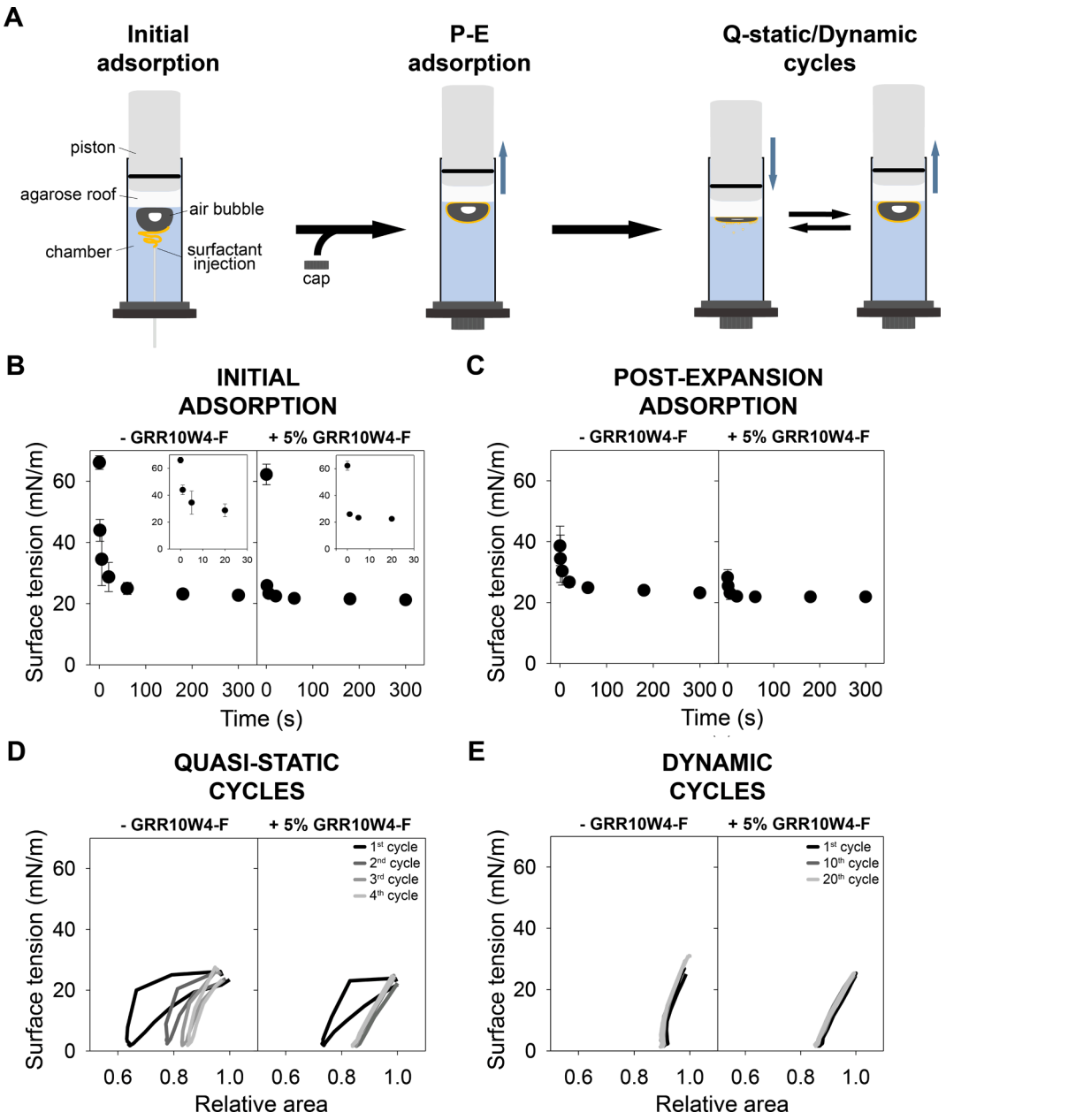

Fig. 3. Effect of GRR10W4-F on the interfacial behaviour of surfactant tested in the CBS. (A) Graphical scheme of a captive bubble surfactometer (CBS) experiment. Surface tension-time isotherms during (B) initial and (C) post-expansion adsorption kinetics of an aqueous suspension from OE in the absence or in the presence of 5 mass% peptide/total phospholipids of peptide GRR10W4-F. Insert shows an expansion of the first 30 s of initial adsorption. Data represents the average and standard deviation from three different experiments. (D) Comparison of the performance of interfacial films formed by OE suspensions in the absence or in the presence of GRR10W4-F, during 4 slow quasi-static cycles and (E) 20 rapid dynamic compression-expansion cycles. A representative γ-area isotherm of three experiments is shown, including the four quasi-static cycles and the 1st, 10th and 20th dynamic cycles.

similar isotherms for peptide-loaded and peptide-free OE, in both cases with a non-hysteretic character, showing the notable behaviour of OE under these conditions. Taken together, these observations show that the peptide does not detrimentally affect surfactant function but actually improves its interfacial performance, possibly by enhancing material refining at the air–water interface.

3.3. *Interfacial delivery of GRR10W4-F by pulmonary surfactant*

Next, we investigated the ability of PS membranes to efficiently incorporate the peptide GRR10W4-F, transporting and delivering it throughout air–liquid interfaces. In order to mimic the respiratory interface *in vitro*, we used a double-balance setup with both donor and recipient compartments, connected by an interfacial bridge, also introducing compression-expansion dynamics at the recipient surface to study their effect on the vehiculization of PS/GRR10W4-F films (Fig. 4**A**).

3.3.1. *Interfacial vehiculization of GRR10W4-F by different surfactant preparations*

First, we evaluated the vehiculization of GRR10W4-F by different surfactant preparations over a clean air–liquid interface. NS membrane complexes, OE MLVs, or the clinical surfactant Csf were combined with 5 mass% GRR10W4-F, and injected into the donor of the double-balance setup. Fig. 4**B** shows the surface pressure–time isotherms derived from the adsorption and spreading of surfactant samples, in the absence (left

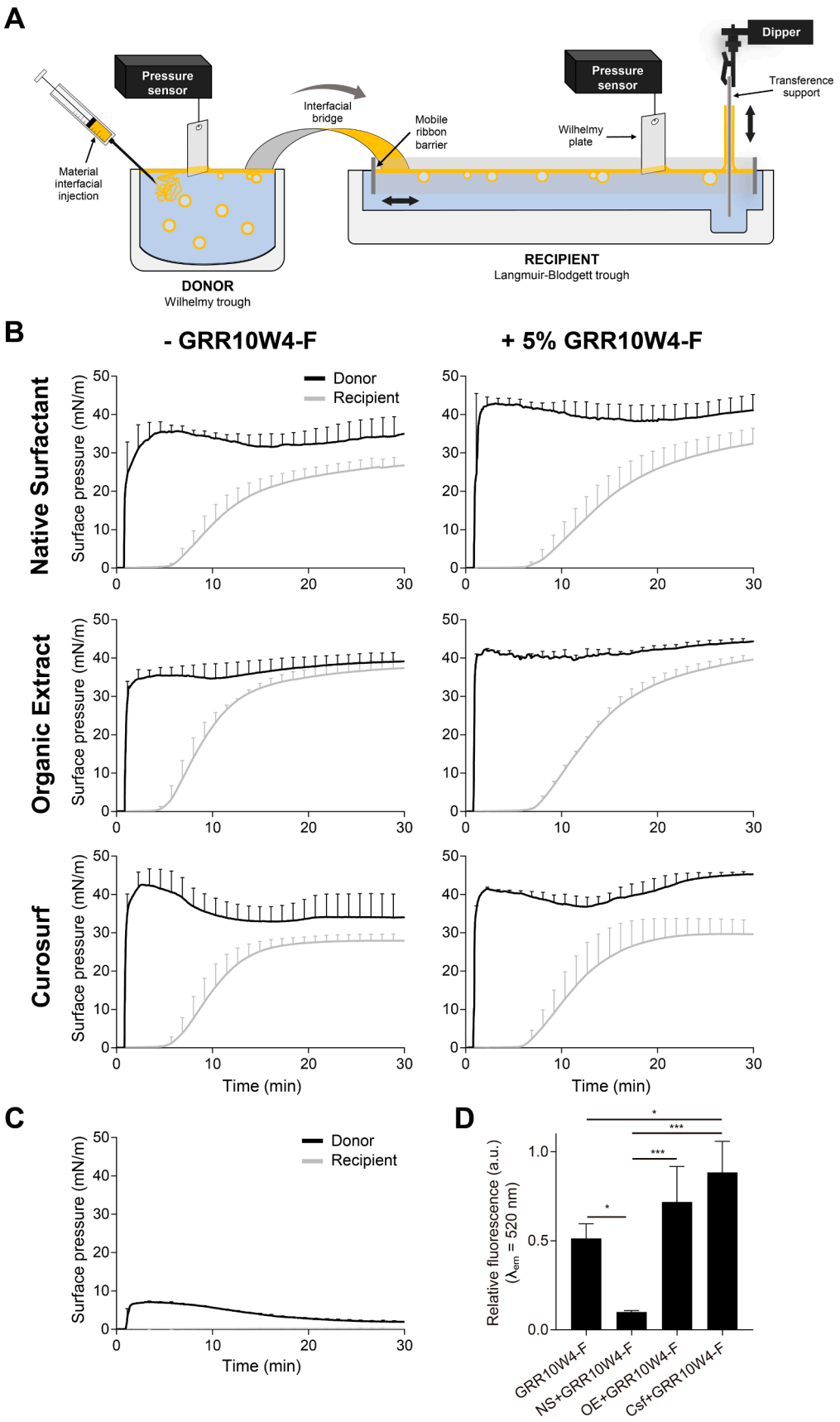

Fig. 4. Interfacial vehiculization of GRR10W4-F by pulmonary surfactant preparations. (A) Schematic illustration of the double-balance setup used in the vehiculization experiments, combining a Wilhelmy with a Langmuir-Blodgett balance. (B) Π-time isotherms comparing the adsorption/spreading behaviour of NS (top), aqueous suspension of OE (middle) and Curosurf® (bottom) in the absence (left column) or in the presence (right column) of GRR10W4-F (5 % w/w with respect to the total mass of phospholipids). Black (donor) and grey (recipient) lines and bars represent the mean and standard deviations, respectively, obtained from three independent replica. (C) Adsorption/spreading isotherm upon injection of 15 μL at 900 μM of GRR10W4-F (control of 5 % w/w with respect to the mass of phospholipids) at the donor compartment. (D) Relative fluorescence emission of GRR10W4-AlexaFluor488 ($\lambda_{em} = 520$ nm), corrected in reference to the corresponding fluorescence intensity yield in the different environments, present in the material from the recipient interface collected by aspiration at the end of each experiment. All samples were measured under the same sensitivity to allow the comparison of the results. Data represent mean and standard deviation calculated from three different experiments. One-way ANOVA ($p < 0.001$) followed by Tukey post-hoc test: (*) $p < 0.05$ and > 0.01, and (***) $p \leq 0.005$.

panels) or in the presence (right panels) of the peptide. The deposition of each of the materials at the donor interface produced an immediate increase in surface pressure in that compartment, which was transmitted to the recipient trough after around 5 min. This increase in surface pressure in the recipient compartment produced a slight decrease in the donor trough, likely derived from the transference of material between both compartments. The combination of 5 mass% GRR10W4-F with NS, reconstituted OE, or Csf, resulted in all cases in an improvement of the adsorption capabilities of surfactant, perceptible as a higher increase in the surface pressure values reached at the donor trough. These observations are in accordance with the previous results obtained for the adsorption of MLVs and OE at the CBS. However, the spreading properties seem to be slightly affected, as the surface pressure in the recipient compartment started to increase 1–2 min later in the experiments where the peptide was present. This could indicate that the intercalation of GRR10W4-F into PS films reduces somehow membrane fluidity and, therefore, affects the diffusion capabilities. The interfacial deposition of GRR10W4-F alone (Fig. 4**C**) produced an instantaneous rise in the surface pressure to values of ~ 5–7 mN/m that decayed over time, probably due to the spreading to the recipient trough, even though the surface pressure did not increase in this compartment, possibly by desorption and subsequent dilution of the peptide into the large subphase of the recipient compartment. Thirty min after sample injection, the bridge was removed to prevent the transference of more material from the donor trough, and the interfacial material at the recipient trough was collected by aspiration, to subsequently measure the fluorescence associated to the fluorescent dye. The yield fluorescence intensity, derived from the fluorescence intensity of GRR10W4-F assessed under comparative conditions in the different surfactant environments, was first evaluated. A significant reduction of the fluorescence was observed in the AMP alone and combined with NS with respect to Csf, being NS the preparation that seems to reduce more the detection of the signal, as observed in **Figure S2** (available in https://doi.org/10.6084/m9.figshare.20747824). Therefore, all fluorescence measurements were corrected taking into account this factor. As summarized in Fig. 4**D**, the peptide alone was capable to spread to the recipient trough as we were able to detect its fluorescence. However, when GRR10W4-F was combined with NS, this signal was drastically reduced and we were not able to detect almost any fluorescence for these samples reaching the recipient compartment. On the contrary, the amount of fluorescence that was detected was significantly improved when it was combined with reconstituted OE or with Csf.

3.3.2. *GRR10W4-F vehiculization over surfactant-occupied interfaces*

In order to approximate the experimental conditions to the physiological situation in the lung, we also performed experiments in which the interface was previously occupied by PS. For this, a minimal quantity of NS (1 μL at 50 mg/mL) was injected at the donor interface to coat both donor and recipient interfaces, but avoiding the formation of surface-associated reservoirs, as this would cause adsorption and spreading of new material. After 30 min of equilibration and once a surface pressure of ~ 20 mN/m was reached, 15 μL GRR10W4-F alone or pre-mixed with 50 mg/mL Csf (5 % peptide-to-lipid mass ratio) were injected into the donor interface. Fig. 5**A-B** illustrates the typical sharp increment in surface pressure at the donor trough occurring after the addition of GRR10W4-F alone or combined with Csf. The material travelling to the recipient trough caused a slight increase in the recipient surface pressure (2.5 ± 0.8 mN/m upon injection of the AMP alone, and 6.3 ± 2.4 mN/m when combined with Csf). Thirty min after this second injection, the interfacial film at the recipient trough was collected by aspiration. Finally, the fluorescence of the dye conjugated to the peptide was measured to determine the vehiculization of GRR10W4-F over surfactant-occupied interfaces. This fluorescence was again corrected by the yield fluorescence intensity of GRR10W4-F in each preparation (**Figure S2**, https://doi.org/10.6084/m9.figshare.20747824). As observed in Fig. 5**C**, the peptide alone was able to spread readily even though the interface was previously occupied by PS, but this transference was higher when combined with Csf. Also demonstrating the efficiency of the combined system containing the peptide, there were no significant differences comparing the fluorescence obtained in experiments performed over clean with that recorded in experiments with interfaces pre-coated by NS.

3.3.3. *Effect of dynamic breathing-like cycles on GRR10W4-F release*

Having confirmed that PS is capable of transporting GRR10W4-F over both clean and surfactant-occupied interfaces, we next studied the effect of introducing interfacial breathing-like dynamics on the delivery of material. Using the same double-balance setup, we compared the effect of compression-expansion cycles on the spreading of OE in the absence or in the presence of GRR10W4-F, and how these cycles could promote the release of the peptide from the interface once vehiculized. As no significant differences were observed in the AMP vehiculization by Csf or OE, we used the latter as it has been largely characterized by our group as well as to facilitate a better and more controlled labelling of the sample. An aqueous suspension of OE (15 μL at 50 mg/mL) was deposited dropwise into the donor interface, producing a rapid increase

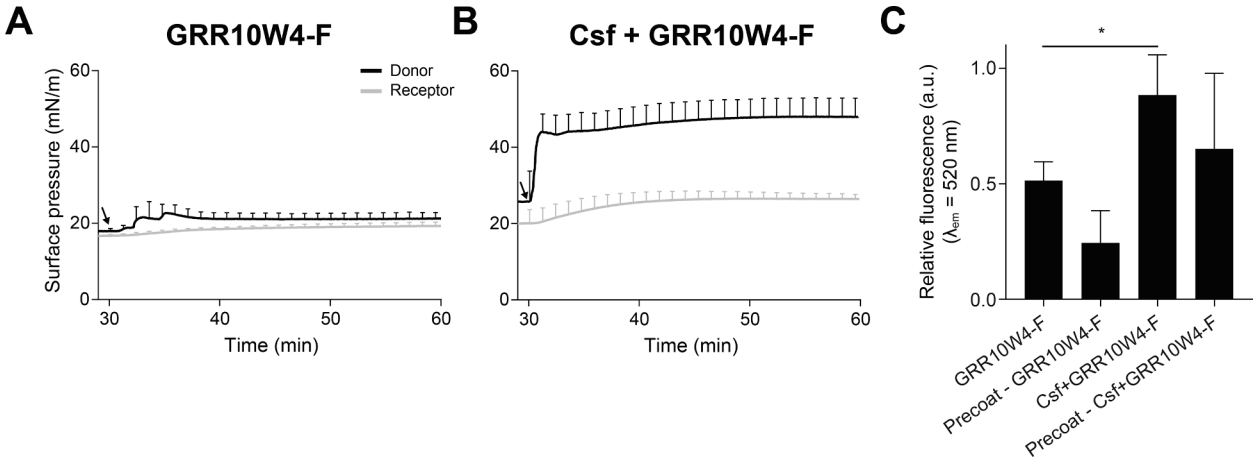

Fig. 5. Interfacial vehiculization of GRR10W4-F across surfactant-occupied interfaces. Adsorption/spreading isotherms of (A) GRR10W4-F and (B) Curosurf® (Csf) combined with 5 % w/w GRR10W4-F injected (black arrows) into the interface 30 min after covering it with an interfacial film of NS. (C) Relative fluorescence emission of GRR10W4-AlexaFluor488 (λ_{em} = 520 nm) present at the recipient interface at the end of each experiment, corrected in reference to the corresponding fluorescence intensity yield in the different environments. The fluorescence obtained from experiments performed over clean interfaces are also included in this graph for comparison. Data are average and standard deviation of 3 independent experiments. Unpaired *t*-test (*) $p < 0.05$.

in the donor surface pressure (Π) and, around 5 min later, in the recipient compartment, as described in the previous static experiments. Then, 10 compression-expansion cycles were performed in the recipient compartment 30 min after the injection of OE or OE + GRR10W4-F. Fig. 6**A-B** shows the Π-area isotherms of the 1st, 5th and 10th cycle performed for each sample. The typical exclusion plateau of surfactant at surface pressures of 45–50 mN/m was observed for both samples, especially for the first cycle, and it was gradually reduced along the cycles. In the isotherms of peptide-free OE, the length of this plateau was just slightly reduced over the following cycles. Interestingly, the presence of the peptide produced a shorter plateau in the first cycle, which suffered a more pronounced reduction during cycles, practically

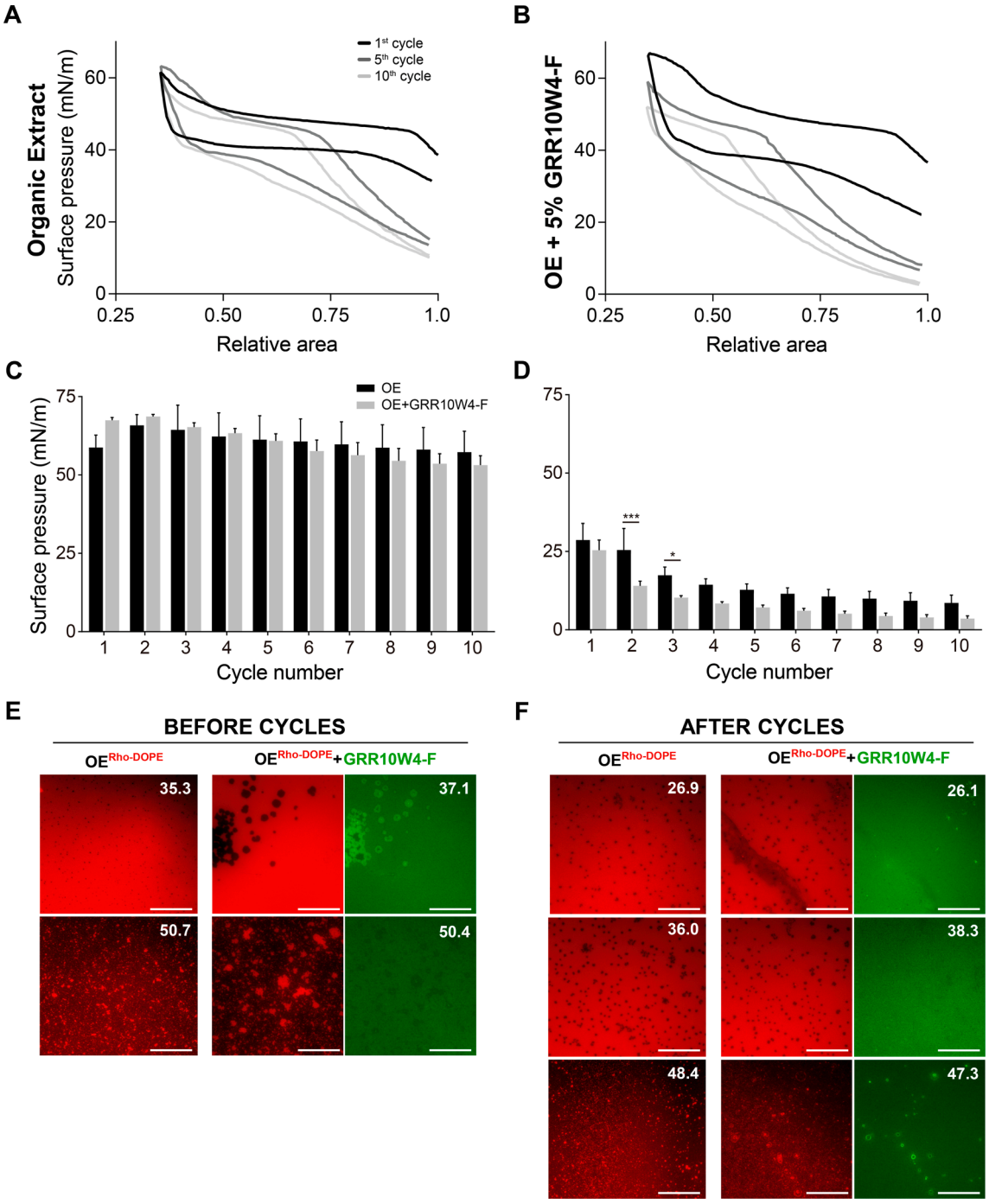

Fig. 6. Interfacial release and distribution of GRR10W4-F during interfacial compression-expansion dynamics. (A) Π-area isotherms of the 1st, 5th and 10th compression-expansion cycles performed on OE films doped with Rho-DOPE, upon vehiculization and after removing the interfacial bridge. (B) Π-area isotherms of the 1st, 5th and 10th compression-expansion cycles performed in the recipient compartment after the vehiculization of OE/Rho-DOPE + GRR10W4-F. In both A and B, one representative experiment is shown. (C) Maximal and (D) minimal surface pressure reached along the different compression-expansion cycles. Mean and standard deviation were calculated from 3 different experiments. Two-Way ANOVA min cycles (cycles: $p < 0.001$, peptide: $p < 0.001$), Tukey post-hoc test: (*) $p < 0.05$ and > 0.01, and (***) $p \leq 0.005$. (E, F) Epifluorescence images comparing films of OE/Rho-DOPE (left) or OE/Rho-DOPE + GRR10W4-F (right) transferred onto glass coverslips before (E) or after (F) being subjected to compression-expansion cycles and observed under an epifluorescence microscope. The surface pressure value corresponding to each image is indicated in upper right corners. Red images: fluorescence from Rho-DOPE; green images: fluorescence from GRR10W4-F. Scale bar: 25 μm.

disappearing for the expansion step of the 10th cycle. Fig. 6**C-D** illustrates the decay of maximal and minimal surface pressures, respectively, reached along the cycles. After the first compression, only OE in combination with 5 % GRR10W4-F reached the highest surface pressure values (~70 mN/m), meaning surface tension values near collapse, i.e. close to 0 mN/m. However, this surface pressure was more pronouncedly reduced over cycles in the presence of peptide. In the absence of GRR10W4-F, PS needed at least two cycles of compression in order to reach surface pressures near collapse, but these values were reduced more slightly along the cycles. The minimum surface pressure showed a similar trend, as it decreased along the cycles, the reduction again being more pronounced in OE films containing GRR10W4-F than in films of OE alone.

To complete these experiments, we doped OE with a fluorescent probe, Rho-DOPE, to additionally analyse the lateral structure of the vehiculized lipid film and the distribution of the peptide over it, both before and after subjecting the interface to 10 compression-expansion cycles. Epifluorescence microscopy images (Fig. 6**E-F**) revealed the formation of typical dark condensed domains starting from pressures of 15 mN/m, specially upon cycling, likely as a consequence of the lateral reorganization of the lipids and the exclusion of the more fluid lipids and the probe from the liquid ordered regions. Interestingly, GRR10W4-F appeared widely distributed along the fluid region of the lipid film but being somehow more concentrated in black areas corresponding to domains of peptide exclusion, partly disappearing after subjecting the film to cycling (Fig. 6**F**). In line with the findings above, the intensity of peptide fluorescence decreased over compression and upon cycling. Cycles seem to also homogenize peptide distribution over the film prior to its release from the interface, as can be seen in Fig. 6**F**, at high surface pressures (~50 mN/m). At these pressures, small clusters of the lipid dye Rho-DOPE were formed, which correspond to areas of lateral and interfacial exclusion, surrounded by darker background, indicating that the continuous phase at this lateral pressures is in L_o state and the dispersed phase is in L_d state. However, these structures were not observed in the green channel, where GRR10W4-F appears distributed over the entire compressed film, although apparently partly excluded from the liquid disordered domains. It cannot be discarded that the decrease in peptide fluorescence could be due at least in part to a quenching effect as a consequence of compression-driven accumulation/segregation of the peptide at certain locations preceding exclusion from the surface. After the compression-expansion cycles, the L_o domains appeared smaller and presented high intensity of both AMP and lipid dye, likely connected with the formation of areas of interfacial exclusion, as observed and described previously [26]. These observations indicate that the lateral distribution of Rho-DOPE and GRR10W4-F are completely different, in contrast to what could be expected based on the presence of the bulky fluorescence tag of the peptide, which could exhibit similar phase behaviour as the unsaturated lipids, like the dye Rho-DOPE. No distinct differences were observed in the surfactant film structure when the peptide was present or not, especially after cycling, confirming that the peptide does not have a negative impact on both PS function and structure.

3.4. GRR10W4-F antimicrobial activity and cytotoxicity effect upon combination with PS

To obtain a first indication on how PS binding influences the antimicrobial effects of GRR10W4-F, we evaluated the antimicrobial

A

Material	MIC (μM)
OE	> 40
GRR10W4-F	20
OE+GRR10W4-F	10

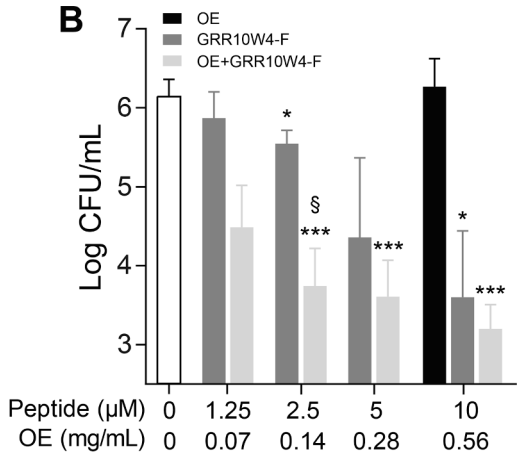

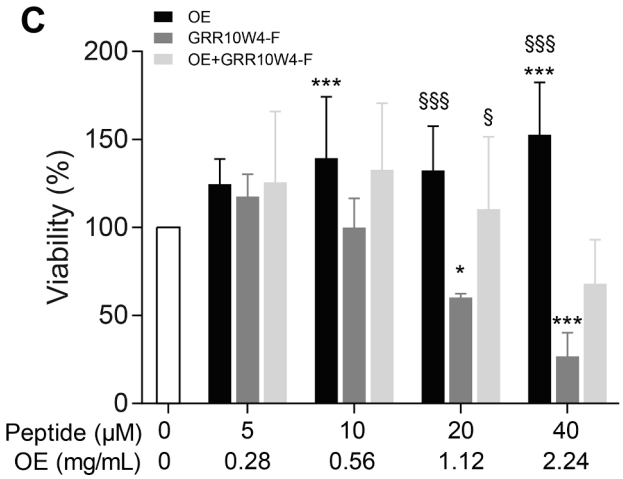

Fig. 7. Antimicrobial activity and cytotoxic effect of GRR10W4-F in the presence of surfactant. Antimicrobial activity of GRR10W4-F against *E. coli* ATCC25922 in the absence and presence of OE, as well as for OE alone, as determined by (A) minimum inhibitory concentration (MIC) and (B) viable count assay (VCA). No bacterial growth was defined as a bacterial concentration of < 1000 CFU/mL (the lowest detectable threshold). Data show mean and SD of 5 independent experiments. One-way ANOVA ($p < 0.001$) followed by Tukey post-hoc test: (§) $p = 0.051$ (Control vs GRR10W4-F 1.25 μM) and $p = 0.068$ (GRR10W4-F 1.25 μM vs OE + GRR10W4-F 1.25 μM), (*) $p < 0.05$ and > 0.01, and (***) $p \leq 0.005$. (C) Viability of human alveolar epithelial cells A549 exposed to different concentrations of GRR10W4-F alone or combined with OE, determined by WST-1. The concentration of OE varies to maintain the same peptide ratio of 5 mass%. Mean and SD calculated from 3 experiments are represented. Two-Way ANOVA (material: non-significant, concentration: $p < 0.001$, interaction concentration × material: $p < 0.001$), Tukey post-hoc test: (*) $p < 0.05$ and > 0.01, and (***) $p \leq 0.005$. (*) designate the comparison with the control of no treatment, while (§) refer to the comparison with the effect of GRR10W4-F alone at the same concentration.

activity of GRR10W4-F when combined with PS. For this, OE was selected as the reference PS preparation due to the absence of hydrophilic proteins, as they could add an extra antimicrobial effect [45,46]. As shown in Fig. 7**A-B**, OE suspensions did not present antimicrobial activity by themselves at the maximum concentration tested, as evidenced by both MIC and VCA results. In contrast, combining 5 mass% GRR10W4-F with OE MLVs lead to increased antimicrobial activity over *E. coli* ATCC 25922 compared to that of peptide alone, based on the significantly lower MIC obtained for the OE + AMP combination (see Fig. 7**A**). These results were confirmed by VCA assays, which showed that the incorporation of GRR10W4-F into OE membranes significantly improved the antimicrobial effects at peptide concentrations from 2.5 μM and above (Fig. 7**B**). While thus displaying promising antimicrobial effects, the combination of PS and GRR10W4-F induced only moderate toxicity on lung cells compared with GRR10W4-F alone. Thus, for cultures of A549, an ATII-derived cell line, as a simple model of airway epithelial cells, only minor cytotoxic effects were observed at peptide concentrations $\leq$ 20 μM (as shown in Fig. 7**C**). A slightly higher cytotoxicity was observed at 40 μM peptide. When combined with OE, GRR10W4-F displayed lower cytotoxic effect than the peptide alone at any of the concentrations tested, suggesting a certain protective role of OE for lung epithelial cells exposed to AMPs. OE also exhibited no negative effect on cell viability by itself, even at the highest concentration tested.

4. Discussion

In the current work, the capability of different pulmonary surfactant models and clinical formulations to deliver the antimicrobial peptide GRR10W4-F through air–liquid interfaces has been evaluated in detail. The emergence of AMPs has opened new possibilities towards the fight against MDR bacteria and persistent infections. One of the main challenges in the use of these therapeutic molecules is, however, to overcome the low bioavailability at the site of infection, especially for the treatment of LTRIs [11,47]. In order to address this problem, we have studied by different *in vitro* models the possibility to incorporate the AMP GRR10W4-F into PS formulations to improve the transport of the peptide over the air–water interface, which could potentially facilitate its access to the distal airways.

The incorporation of AMPs into exogenous PS for airway delivery has been proposed previously by Banaschewski *et al.* [22], who evaluated the incorporation of four different cathelicidin peptides into a clinical surfactant preparation. While a detrimental effect on both antimicrobial and surfactant biophysical activities were observed for three out of the four peptides tested, the combination of Cathelicidin-2 with PS showed good biophysical and antimicrobial performance [22,27,28]. However, the peptides used in that study did not present any protein engineering modification, such as hydrophobic end-tags, which have been previously demonstrated to enhance lipid membrane interactions and antimicrobial effect of AMPs [29,30]. Addressing this, GRR10W4-F was found here to be able to adsorb by itself at the air–liquid interface and form a stable film in a concentration-dependent manner, similar to other amphiphilic peptides (Fig. 1**B-C**). The same interfacial activity is likely defining the propensity of GRR10W4-F to insert also into lipid monolayers and PS-like films (Fig. 2**A**), in line with previous findings for other bilayers of different phospholipid compositions [30]. The insertion of GRR10W4-F into POPG or DPPC:POPC:POPG:Chol films led to Π_c values around 30 mN/m. Considering that the lateral packing of phospholipids in biological membranes is equivalent to that achieved at surface pressures in the range of 30–35 mN/m [48], our results indicate that GRR10W4-F could penetrate into lipid bilayers, as long as these contain anionic and unsaturated phospholipids. The results observed here are consistent with what was previously described for this peptide [30], which presents reduced insertion into zwitterionic compared with anionic membranes, and similarly in the presence of cholesterol. The influence of the AlexaFluor488 dye on the interfacial activity of this peptide should be further investigated, as previous investigators have described an increased membrane permeabilization, altered membrane organization and reduced cytotoxicity of cell-penetrating peptides labelled with small aromatic fluorophores [49,50]. However, a prior work investigating the binding of GRR10W4 and GRR10W4-F to melanoma cell membranes that demonstrated good correlation between binding, cell membrane permeation and cell toxicity between both AMP versions [51], together with the considerably low membrane interaction factor described for this fluorophore [52] suggest that the effect of the labelling is less important for the correlation and that our observations are mainly due to the W-tag attached to this AMP. Epifluorescence images (Fig. 6**E-F**) reveal that the peptide is widely spread in surfactant films at surface pressures $\leq$ 50 mN/m, especially before reaching extreme compression, indicating its efficient insertion into PS films at surface pressures above the threshold for insertion into lipid bilayers. The interaction with lipids is also the reason for the improved interfacial adsorption observed when MLVs containing the hydrophobic surfactant proteins SP-B and SP-C were combined with different versions of this AMP (Fig. 2**B-C**). As expected, the incorporation of SP-B and SP-C was essential for an efficient transfer of phospholipids out from membranes into the interface [21,53,54]. This improvement on adsorption capabilities, strictly dependent on the presence of the hydrophobic surfactant proteins, could indicate a possible interaction between the peptide and the proteins, and/or a combined or synergistic action of peptide and proteins. The peptide without the hydrophobic tag, GRR10, was able to slightly enhance PS-like MLVs adsorption, but the incorporation of the tryptophan-tag and, even more, the tag plus the Alexa fluorophore, significantly increased the surface pressure obtained upon vesicle injection, clearly pointing to the importance of hydrophobic domains for this. One of the antimicrobial modes of action of AMPs is associated with membrane perturbation and rupture, which is likely potentiated in the presence of the hydrophobic end-tag [30,31,55]. This, in turn, may trigger conversion of MLVs into smaller vesicles, with higher interfacial activity [56]. The formation of green bright spots, likely enriched in AMP, observed here by epifluorescence after compression of interfacial films (Fig. 6**F**) could be also connected to this structural transition, in this case from a monolayer to bilayer vesicles or reservoirs excluded from the interface by lateral compression. These results demonstrate the important role of the W-tag in the observed improved capabilities of PS along this study, but also that there is still room for further optimization, as illustrated by the boosting effect of the Alexa488 dye. Future studies are therefore needed to explore the window of possibilities to improve this or other AMPs in order to enrich the PS properties that can facilitate the interface-assisted vehiculization of this type of peptides.

Overall, the incorporation of 5 % w/w of GRR10W4-F does not seem to detriment the main biophysical properties of PS, as observed both by CBS (Fig. 3) and surface balances (Figs. 4 and 6). In fact, incorporation of GRR10W4-F improves interfacial adsorption properties of OE and different PS-like lipid mixtures, again likely due to the intrinsic interfacial activity of the peptide and the membrane interactions mediated by its W-tag and the attached fluorophore. As observed both in Langmuir balance (Fig. 6) and CBS (Fig. 3), loading OE with 5 % GRR10W4-F led to shorter plateaus and reduced hysteresis during compression-expansion cycles, likely associated with partial loss of interfacial material over cycles, potential compositional refining and/or structural rearrangements at the interfacial film, and possibly a more dynamic character. These observations provide evidence of peptide interaction and incorporation into PS films while not damaging, but rather improving, its biophysical function. This 5 mass% AMP used in the whole study was the minimum necessary to detect vehiculization mediated by NS, so as it was not affecting the biophysical function of PS and was perfectly detected upon the vehiculization with OE and Curosurf®, we choose this percentage for comparison and consistency between all the different experiments.

Conversely, many studies have reported the efficiency and advantages of using PS to transport different therapeutic molecules along the

respiratory surface, such as hydrophobic drugs [26,57], antibiotics [24,58], proteins [25] or small-interfering RNA [23,59]. However, only recently, the ability of surfactant to use the air–liquid interface as a delivery route has been explored [60]. After confirming the interaction between GRR10W4-F and PS and establishing that the presence of the peptide does not significantly affect surfactant function, we determined that its incorporation into surfactant complexes allows in fact an improved peptide transport along air–liquid interfaces (Figs. 4 and 5). Surfactant preparations with simplified composition and structure, like OE or Csf, can transport the peptide along the interface more efficiently than more complex materials like NS, and much more efficiently than delivering the peptide alone. GRR10W4-F did not apparently insert into full NS films and was not vehiculized. Apparently, the preferential adsorption of the compositionally heterogeneous NS at the interface prevented the adsorption and spreading of the peptide. In contrast, our result indicate that GRR10W4-F competes successfully with OE and Csf membranes for the air–water interfaces. As a consequence, the peptide is interfacially delivered from the donor to the recipient compartment. Quantitatively, Csf seems to carry the peptide slightly more efficiently than OE, likely an effect due to the absence of cholesterol, which has previously been found to substantially reduce incorporation of GRR10W4 into phospholipid membranes [30].

The success of a delivery strategy does not only depend on the capability of the vehicle to transport the therapeutic molecule, but also on the subsequent release and effective action on reaching the target site. The respiratory system is a highly dynamic environment where the operative surface area is continuously compressing and expanding during the breathing cycles. These compression-expansion dynamics have demonstrated to promote selective interfacial exclusion of unsaturated lipids and other related molecules that cannot sustain high compression rates [19,20,26]. Here, we have obtained evidence for a progressive release of GRR10W4-F from the interface during compression-expansion cycles of the interfacial PS films using both CBS (Fig. 3) and Langmuir-Blodgett balance (Fig. 6). Our results suggest that the bulky hydrophobic tag, including the attached fluorophore, allow insertion of the peptide into OE layers, increasing packing and pressure, facilitating maximum surface pressure or minimal surface tension already on the first compression and making the film less foldable. However, due to its bulkiness, GRR10W4-F does not support large compression and tight lateral packing. Instead, it promotes rapid exclusion during the first compression, improving film refining and leading to the reduction of both maximum and minimum surface pressures through the cycles. The aromatic residues in proteins and peptides have high affinity for polar/non-polar interfaces and a strong tendency to penetrate by 2.5–8 Å into lipid membranes, maintaining association with the polar headgroup region of phospholipids [8]. The peptide could also participate in the insertion of further surface-active lipids to compensate those that are lost as a consequence of collapse along the plateau. This allows the material excluded from the interfacial film to maintain its surface association, forming surface-associated membrane reservoirs available for re-adsorption and re-spreading, contributing to the good dynamic behaviour of PS [53,61]. The penetration of the peptide into lipid surfaces may in this case be potentiated by the presence of the Alexa488 dye, as evidenced by the improved interfacial adsorption of vesicles in comparison with the GRR10W4 peptide without this fluorophore. Furthermore, at a peptide concentration above certain threshold, this may trigger membrane disruption by inducing negative curvature and promoting formation of micelles [7,29,31,32,62]. We hypothesize that these modes-of-action for membrane perturbation by peptides, together with the hypothesized exclusion of the rigid tag from the most condensed states reached by surface films during compression, enable a rapid exclusion of the peptide from the interface, either alone or associated with some lipids, also facilitating the formation of three-dimensional structures associated to the interface. This is consistent with our epifluorescence results (Fig. 6**E-F**), in which GRR10W4-F appears homogeneously distributed over the film, consistent with the carpet model [7,30,62], but seems more concentrated in the L_o domains following lateral compression. The detection of some black regions in the red channel that appears with intense fluorescence in the green channel could correspond to nucleation points concentrating the peptide, which would initiate the disruption of the surface layers and the interfacial exclusion. Based on all this, we propose that the presence of the peptide could trigger the formation of 3D structures still in contact with the interfacial layer, as we can detect surface-associated peptide fluorescence. At the highest surface pressures and, especially upon compression-expansion cycling, the peptide fluorescence intensity decreases at pressures above 45–50 mN/m, indicating the ultimate interfacial exclusion of the peptide. Although this reduction in fluorescence intensity is in accordance with the results obtained with the CBS and the Langmuir balance, and suggest an interfacial exclusion of the peptide, we cannot at this point exclude a possible self-quenching or quenching of the fluorophore due to the proximity with tryptophan [63,64], potentiated as a consequence of the accumulation upon compression. As mentioned above, it is remarkable that the lateral exclusion of the lipid probe Rho-DOPE does not follow the same pattern, suggesting that the peptide follows its own pattern of lateral segregation and three-dimensional exclusion. These results could be confirmed or complemented by carrying out similar analysis performed with GRR10W4 versions labelled at the *N*-terminal region, to determine whether these observations are due to the particular behaviour caused by the combination in close proximity of the dye and the W-tag.

Finally, we determined that GRR10W4-F retained its antimicrobial capability when combined with lung surfactants based on both MIC and VCA assays performed on *E. coli* ATCC 25922 (Fig. 7**A-B**) and being even more effective than the peptide alone especially at low peptide concentrations. If the W-tag is the motif that facilitates peptide insertion into surfactant membranes, its cationic residues would be still available to interact with the anionic lipids in bacterial membranes. This effect is expected to be further enhanced in the presence of a hydrophobic fluorescent dye as in GRR10W4-F, in line with previous findings of fluorescent labelling enhancing membrane binding and destabilization of both model lipid membranes and bacterial membranes [49,50]. Adding to this, we speculate that surfactant vesicles might promote a first contact with the bacterial membrane, facilitating the subsequent interaction and partitioning of GRR10W4-F, thereby improving the antibacterial effect of the formulation. Moreover, a synergistic action of the AMP together with the surfactant proteins can also occur *in vivo*, based on the intrinsic antibacterial and anti-inflammatory action of the proteins [65–68] and the cooperative action observed for SP-A with an AMP [69]. Preliminary experiments confirmed that this effect was not accompanied of a significant cytotoxic effect toward mammalian cells [4,11], also confirmed here for pulmonary A549 cells (Fig. 7**C**). However, in the further exploration of the potential of translation of these types of systems towards therapeutics, experiments should be extended to test bacterial killing against other bacterial strains, especially true pulmonary pathogens, and using other antibacterial assays, as well as complementing cytotoxicity assays towards different cell types, evaluating the effect of GRR10W4-F after its vehiculization, and to finally confirm these results using an *in vivo* model.

To summarize, the data presented in this study point to potential benefits of employing exogenous surfactant preparations as a delivery vehicle for inhaled administration of hydrophobically end-tagged AMPs. We demonstrated that the incorporation of the peptide GRR10W4-F into surfactant membranes does not detrimentally affects surfactant biophysical functions, which is expected to be important not only for the surfactant used as a vehicle but also for the subsequent interaction with the endogenous PS once delivered into the lungs. Furthermore, the combination of GRR10W4-F with clinical surfactant could potentially enhance the distribution of the peptide over the respiratory interface while opening collapsed lung areas affected by the infection, increasing the effective concentration at the infection site. Apart from the GRR10W4-F function presented here, other drugs could potentially be

also simultaneously combined for lung therapy, including anti-cancer or anti-inflammatory peptides, some of which have been found to display boosted biological effects as a result of W-tagging [51,70], or other adjuvant molecules that could improve the uptake of small drugs by pathogens or malignant cells [51,55]. This work also suggests that the inclusion of hydrophobic tags into other therapeutic proteins, such as antibodies, could facilitate their interaction with PS and improve its administration into the lungs. Clearly, the models used in the present study are still far from the *in vivo* scenario and much additional work is needed to assess how AMPs and PS are optimized and what consequences such optimization has on the wider biological performance of such systems. Moreover, the impact and vehiculization of higher percentages of the AMP should be investigated to determine whether it does not still affect PS properties and enhances the vehiculization and antimicrobial activity, with no substantial cytotoxicity. Reproducing these experiments with GRR10 and GRR10W4, or with other modified versions of the peptides, would strengthen the significancy of this study as it would help to determine the contribution of the W-tag in the vehiculization and biological activity of the AMP. The continuation of this study to explore closer to *in vivo* scenarios will precede the potential transfer of PS/GRR10W4 formulations into clinical contexts.

Declaration of Competing Interest

The authors declare that they have no known competing financial interests or personal relationships that could have appeared to influence the work reported in this paper.

Acknowledgements

This work has been funded by the Spanish Ministry of Science and Innovation (RTI2018-094564-BI00, PID2021-124932OB-I00) and the Regional Government of Madrid (P2018/NMT-4389). CG-M acknowledges an FPU fellowship (Ref. FPU16/02553) from the Spanish Ministry of Education, Culture and Sport.

References

[1] A. Fleming, On the antibacterial action of cultures of a penicillium, with special reference to their use in the isolation of B. influenzae, Brit. J. Exp. Pathol. 10 (1929) 226–236.
[2] M. Drayton, J.P. Deisinger, K.C. Ludwig, N. Raheem, A. Müller, T. Schneider, S. K. Straus, Host Defense Peptides: Dual Antimicrobial and Immunomodulatory Action, Int. J. Mol. Sci. 22 (2021) 11172.
[3] R.I. Aminov, A brief history of the antibiotic era: lessons learned and challenges for the future, Front Microbiol 1 (2010) 134.
[4] M. Pasupuleti, A. Schmidtchen, M. Malmsten, Antimicrobial peptides: key components of the innate immune system, Crit. Rev. Biotechnol. 32 (2012) 143–171.
[5] M. Mahlapuu, J. Håkansson, L. Ringstad, C. Björn, Antimicrobial peptides: an emerging category of therapeutic agents, Front. Cell. Infect. Microbiol. 6 (2016) 194.
[6] R.E. Hancock, H.-G. Sahl, Antimicrobial and host-defense peptides as new anti-infective therapeutic strategies, Nat. Biotechnol. 24 (2006) 1551–1557.
[7] K.A. Brogden, Antimicrobial peptides: pore formers or metabolic inhibitors in bacteria? Nat. Rev. Microbiol. 3 (2005) 238–250.
[8] E. Glukhov, M. Stark, L.L. Burrows, C.M. Deber, Basis for selectivity of cationic antimicrobial peptides for bacterial versus mammalian membranes, J. Biol. Chem. 280 (2005) 33960–33967.
[9] H.-K. Kang, C. Kim, C.H. Seo, Y. Park, The therapeutic applications of antimicrobial peptides (AMPs): a patent review, Journal of microbiology 55 (2017) 1–12.
[10] Y. Luo, Y. Song, Mechanism of Antimicrobial Peptides: Antimicrobial, Anti-Inflammatory and Antibiofilm Activities, Int. J. Mol. Sci. 22 (2021) 11401.
[11] G.S. Dijksteel, M.M. Ulrich, E. Middelkoop, B.K. Boekema, Lessons learned from clinical trials using antimicrobial peptides (AMPs), Front. Microbiol. 12 (2021) 287.
[12] V. Vimberg, K. Buriankova, A. Mazumdar, P. Branny, G.B. Novotna, Role of membrane proteins in bacterial resistance to antimicrobial peptides, Med. Res. Rev. 42 (2022) 1023–1036.
[13] C. Troeger, B. Blacker, I.A. Khalil, P.C. Rao, J. Cao, S.R. Zimsen, S.B. Albertson, A. Deshpande, T. Farag, Z. Abebe, Estimates of the global, regional, and national morbidity, mortality, and aetiologies of lower respiratory infections in 195 countries, 1990–2016: a systematic analysis for the Global Burden of Disease Study 2016, Lancet. Infect. Dis 18 (2018) 1191–1210.
[14] J.J. Iszatt, A.N. Larcombe, H.-K. Chan, S.M. Stick, L.W. Garratt, A. Kicic, Phage Therapy for Multi-Drug Resistant Respiratory Tract Infections, Viruses 13 (2021) 1809.
[15] G. Chen, K. Xu, F. Sun, Y. Sun, Z. Kong, B. Fang, Risk Factors of Multidrug-Resistant Bacteria in Lower Respiratory Tract Infections: A Systematic Review and Meta-Analysis, Can. J. Infect. Dis. Med. Microbiol. 2020 (2020) 7268519.
[16] A. Hidalgo, A. Cruz, J. Pérez-Gil, Barrier or carrier? Pulmonary surfactant and drug delivery, European Journal of Pharmaceutics and Biopharmaceutics 95 (2015) 117–127.
[17] R. Guagliardo, J. Perez-Gil, S. De Smedt, K. Raemdonck, Pulmonary surfactant and drug delivery: Focusing on the role of surfactant proteins, J. Control. Release 291 (2018) 116–126.
[18] J.J. Haitsma, U. Lachmann, B. Lachmann, Exogenous surfactant as a drug delivery agent, Adv. Drug Deliv. Rev. 47 (2001) 197–207.
[19] J. Pérez-Gil, K.M. Keough, Interfacial properties of surfactant proteins, Biochimica et Biophysica Acta (BBA)-Molecular Basis of Disease 1408 (1998) 203–217.
[20] J. Goerke, Pulmonary surfactant: functions and molecular composition, Biochimica et Biophysica Acta (BBA)-Molecular Basis of Disease 1408 (1998) 79–89.
[21] J. Pérez-Gil, Structure of pulmonary surfactant membranes and films: the role of proteins and lipid–protein interactions, Biochimica et Biophysica acta (BBA)-Biomembranes 1778 (2008) 1676–1695.
[22] B.J. Banaschewski, E.J. Veldhuizen, E. Keating, H.P. Haagsman, Y.Y. Zuo, C. M. Yamashita, R.A. Veldhuizen, Antimicrobial and biophysical properties of surfactant supplemented with an antimicrobial peptide for treatment of bacterial pneumonia, Antimicrob. Agents Chemother. 59 (2015) 3075–3083.
[23] L. De Backer, T. Naessens, S. De Koker, E. Zagato, J. Demeester, J. Grooten, S.C. De Smedt, K. Raemdonck, Hybrid pulmonary surfactant-coated nanogels mediate efficient in vivo delivery of siRNA to murine alveolar macrophages, J. Control. Release 217 (2015) 53–63.
[24] A. Van't Veen, D. Gommers, S.J. Verbrugge, P. Wollmer, J.W. Mouton, P.P. Kooij, B. Lachmann, Lung clearance of intratracheally instilled 99mTc-tobramycin using pulmonary surfactant as vehicle, Br. J. Pharmacol. 126 (1999) 1091–1096.
[25] C. García-Mouton, A. Hidalgo, R. Arroyo, M. Echaide, A. Cruz, J. Pérez-Gil, Pulmonary surfactant and drug delivery: an interface-assisted carrier to deliver surfactant protein SP-D into the airways, Front. Bioeng. Biotechnol. 8 (2021) 1556.
[26] A. Hidalgo, C. Garcia-Mouton, C. Autilio, P. Carravilla, G. Orellana, M.N. Islam, J. Bhattacharya, S. Bhattacharya, A. Cruz, J. Pérez-Gil, Pulmonary surfactant and drug delivery: Vehiculization, release and targeting of surfactant/tacrolimus formulations, J. Control. Release 329 (2021) 205–222.
[27] B. Baer, E.J. Veldhuizen, N. Molchanova, S. Jekhmane, M. Weingarth, H. Jenssen, J.S. Lin, A.E. Barron, C. Yamashita, R. Veldhuizen, optimizing exogenous Surfactant as a pulmonary Delivery Vehicle for Chicken Cathelicidin-2, Sci. Rep. 10 (2020) 1–11.
[28] B.J. Banaschewski, B. Baer, C. Arsenault, T. Jazey, E.J. Veldhuizen, J. Delport, T. Gooyers, J.F. Lewis, H.P. Haagsman, R.A. Veldhuizen, The antibacterial and anti-inflammatory activity of chicken cathelicidin-2 combined with exogenous surfactant for the treatment of cystic fibrosis-associated pathogens, Sci. Rep. 7 (2017) 1–15.
[29] M. Malmsten, G. Kasetty, M. Pasupuleti, J. Alenfall, A. Schmidtchen, Highly selective end-tagged antimicrobial peptides derived from PRELP, PLoS ONE 6 (2011), e16400.
[30] A. Schmidtchen, L. Ringstad, G. Kasetty, H. Mizuno, M.W. Rutland, M. Malmsten, Membrane selectivity by W-tagging of antimicrobial peptides, Biochimica et Biophysica Acta (BBA)-Biomembranes 1808 (2011) 1081–1091.
[31] A. Schmidtchen, M. Pasupuleti, M. Mörgelin, M. Davoudi, J. Alenfall, A. Chalupka, M. Malmsten, Boosting antimicrobial peptides by hydrophobic oligopeptide end tags, J. Biol. Chem. 284 (2009) 17584–17594.
[32] M. Pasupuleti, A. Schmidtchen, A. Chalupka, L. Ringstad, M. Malmsten, End-tagging of ultra-short antimicrobial peptides by W/F stretches to facilitate bacterial killing, PLoS ONE 4 (2009), e5285.
[33] H.W. Taeusch, J.B. De La Serna, J. Perez-Gil, C. Alonso, J.A. Zasadzinski, Inactivation of pulmonary surfactant due to serum-inhibited adsorption and reversal by hydrophilic polymers: experimental, Biophys. J . 89 (2005) 1769–1779.
[34] E. Bligh, W. Dyer, Canadian journal of biochemistry and physiology, A rapid method of lipid extraction and purification 37 (1959) 911–917.
[35] G. Rouser, A. Siakotos, S. Fleischer, Quantitative analysis of phospholipids by thin-layer chromatography and phosphorus analysis of spots, Lipids 1 (1966) 85–86.
[36] J. Pérez-Gil, A. Cruz, C. Casals, Solubility of hydrophobic surfactant proteins in organic solvent/water mixtures. Structural studies on SP-B and SP-C in aqueous organic solvents and lipids, Biochimica et Biophysica Acta (BBA)-Lipids and Lipid, Metabolism 1168 (1993) 261–270.
[37] F. Ravera, R. Miller, Y.Y. Zuo, B.A. Noskov, A.G. Bykov, V.I. Kovalchuk, G. Loglio, A. Javadi, L. Liggieri, Methods and models to investigate the physicochemical functionality of pulmonary surfactant, Curr. Opin. Colloid Interface Sci. 55 (2021), 101467.
[38] C. Autilio, J. Pérez-Gil, Understanding the principle biophysics concepts of pulmonary surfactant in health and disease, Archives of Disease in Childhood-Fetal and Neonatal Edition 104 (2019) F443–F451.
[39] D. Schürch, O.L. Ospina, A. Cruz, J. Pérez-Gil, Combined and independent action of proteins SP-B and SP-C in the surface behavior and mechanical stability of pulmonary surfactant films, Biophys. J . 99 (2010) 3290–3299.
[40] S. Schurch, H. Bachofen, J. Goerke, F. Possmayer, A captive bubble method reproduces the in situ behavior of lung surfactant monolayers, J. Appl. Physiol. 67 (1989) 2389–2396.

[41] W.M. Schoel, S. Schürch, J. Goerke, The captive bubble method for the evaluation of pulmonary surfactant: surface tension, area, and volume calculations, Biochimica et Biophysica Acta (BBA)-General Subjects 1200 (1994) 281–290.
[42] L. Wang, A. Cruz, C.R. Flach, J. Pérez-Gil, R. Mendelsohn, Langmuir– Blodgett films formed by continuously varying surface pressure, Characterization by IR spectroscopy and epifluorescence microscopy, Langmuir 23 (2007) 4950–4958.
[43] I. Wiegand, K. Hilpert, R.E. Hancock, Agar and broth dilution methods to determine the minimal inhibitory concentration (MIC) of antimicrobial substances, Nat. Protoc. 3 (2008) 163–175.
[44] M. Lei, A. Jayaraman, J.A. Van Deventer, K. Lee, Engineering Selectively Targeting Antimicrobial Peptides, Annu. Rev. Biomed. Eng. 23 (2021) 339–357.
[45] U. Kishore, T.J. Greenhough, P. Waters, A.K. Shrive, R. Ghai, M.F. Kamran, A. L. Bernal, K.B. Reid, T. Madan, T. Chakraborty, Surfactant proteins SP-A and SP-D: structure, function and receptors, Mol. Immunol. 43 (2006) 1293–1315.
[46] J.C. Pikaar, W.F. Voorhout, L.M. van Golde, J. Verhoef, J.A. Van Strijp, J.F. van Iwaarden, Opsonic activities of surfactant proteins A and D in phagocytosis of gram-negative bacteria by alveolar macrophages, J. Infect. Dis. 172 (1995) 481–489.
[47] N. Mookherjee, M.A. Anderson, H.P. Haagsman, D.J. Davidson, Antimicrobial host defence peptides: functions and clinical potential, Nat. Rev. Drug Discovery 19 (2020) 311–332.
[48] D. Marsh, Lateral pressure in membranes, Biochimica et Biophysica Acta (BBA)-Reviews on, Biomembranes 1286 (1996) 183–223.
[49] D. Birch, M.V. Christensen, D. Staerk, H. Franzyk, H.M. Nielsen, Fluorophore labeling of a cell-penetrating peptide induces differential effects on its cellular distribution and affects cell viability, Biochimica et Biophysica Acta (BBA)-Biomembranes 1859 (2017) 2483–2494.
[50] S.F. Hedegaard, M.S. Derbas, T.K. Lind, M.R. Kasimova, M.V. Christensen, M. H. Michaelsen, R.A. Campbell, L. Jorgensen, H. Franzyk, M. Cárdenas, H. M. Nielsen, Fluorophore labeling of a cell-penetrating peptide significantly alters the mode and degree of biomembrane interaction, Sci. Rep. 8 (2018) 1–14.
[51] D.T. Duong, S. Singh, M. Bagheri, N.K. Verma, A. Schmidtchen, M. Malmsten, Pronounced peptide selectivity for melanoma through tryptophan end-tagging, Sci. Rep. 6 (2016) 1–17.
[52] L.D. Hughes, R.J. Rawle, S.G. Boxer, Choose your label wisely: water-soluble fluorophores often interact with lipid bilayers, PLoS ONE 9 (2014), e87649.
[53] A.G. Serrano, J. Pérez-Gil, Protein–lipid interactions and surface activity in the pulmonary surfactant system, Chem. Phys. Lipids 141 (2006) 105–118.
[54] F. Possmayer, K. Nag, K. Rodriguez, R. Qanbar, S. Schürch, Surface activity in vitro: role of surfactant proteins, Comp. Biochem. Physiol. A: Mol. Integr. Physiol. 129 (2001) 209–220.
[55] M. Pasupuleti, A. Chalupka, M. Mörgelin, A. Schmidtchen, M. Malmsten, Tryptophan end-tagging of antimicrobial peptides for increased potency against Pseudomonas aeruginosa, Biochimica et Biophysica Acta (BBA)-General Subjects 1790 (2009) 800–808.
[56] K. Nag, J. Perez-Gil, A. Cruz, N.H. Rich, K. Keough, Spontaneous formation of interfacial lipid-protein monolayers during adsorption from vesicles, Biophys. J . 71 (1996) 1356–1363.
[57] C. Dani, I. Corsini, S. Burchielli, V. Cangiamila, R. Romagnoli, B. Jayonta, M. Longini, F. Paternostro, G. Buonocore, Natural surfactant combined with beclomethasone decreases lung inflammation in the preterm lamb, Respiration 82 (2011) 369–376.
[58] A. van't Veen, J.W. Mouton, D. Gommers, B. Lachmann, Pulmonary surfactant as vehicle for intratracheally instilled tobramycin in mice infected with Klebsiella pneumoniae, Br. J. Pharmacol. 119 (1996) 1145–1148.
[59] P. Merckx, J. Lammens, G. Nuytten, B. Bogaert, R. Guagliardo, T. Maes, C. Vervaet, T. De Beer, S.C. De Smedt, K. Raemdonck, Lyophilization and nebulization of pulmonary surfactant-coated nanogels for siRNA inhalation therapy, Eur. J. Pharm. Biopharm. 157 (2020) 191–199.
[60] A. Hidalgo, F. Salomone, N. Fresno, G. Orellana, A. Cruz, J. Perez-Gil, Efficient Interfacially Driven Vehiculization of Corticosteroids by Pulmonary Surfactant, Langmuir 33 (2017) 7929–7939.
[61] J.B. de la Serna, R. Vargas, V. Picardi, A. Cruz, R. Arranz, J.M. Valpuesta, L. Mateu, J. Pérez-Gil, Segregated ordered lipid phases and protein-promoted membrane cohesivity are required for pulmonary surfactant films to stabilize and protect the respiratory surface, Faraday Discuss. 161 (2013) 535–548.
[62] D.I. Chan, E.J. Prenner, H.J. Vogel, Tryptophan-and arginine-rich antimicrobial peptides: structures and mechanisms of action, Biochimica et Biophysica Acta (BBA)-Biomembranes 1758 (2006) 1184–1202.
[63] H. Chen, S.S. Ahsan, M.E.B. Santiago-Berrios, H.D. Abruña, W.W. Webb, Mechanisms of quenching of Alexa fluorophores by natural amino acids, J. Am. Chem. Soc. 132 (2010) 7244–7245.
[64] Y. Oka, H. Shishino, Fluorescence Quenching of Alexa Fluor 488-labeled DNA by Complementary Trp-containing PNA Partitioned in Liquid-ordered Domains, Chem. Lett. 46 (2017) 1672–1675.
[65] M.A. Ryan, H.T. Akinbi, A.G. Serrano, J. Perez-Gil, H. Wu, F.X. McCormack, T. E. Weaver, Antimicrobial activity of native and synthetic surfactant protein B peptides, J. Immunol. 176 (2006) 416–425.
[66] E. Crouch, J.R. Wright, Surfactant proteins A and D and pulmonary host defense, Annu. Rev. Physiol. 63 (2001) 521–554.
[67] J. Li, M. Ikegami, C.-L. Na, A. Hamvas, Q. Espinassous, R. Chaby, L.M. Nogee, T. E. Weaver, J. Johansson, N-terminally extended surfactant protein (SP) C isolated from SP-B-deficient children has reduced surface activity and inhibited lipopolysaccharide binding, Biochemistry 43 (2004) 3891–3898.
[68] H. Jin, A.K. Ciechanowicz, A.R. Kaplan, L. Wang, P.-X. Zhang, Y.-C. Lu, R.E. Tobin, B.A. Tobin, L. Cohn, C.J. Zeiss, Surfactant protein C dampens inflammation by decreasing JAK/STAT activation during lung repair, American Journal of Physiology-Lung Cellular and Molecular, Physiology 314 (2018) L882–L892.
[69] J.M. Coya, H.T. Akinbi, A. Sáenz, L. Yang, T.E. Weaver, C. Casals, Natural anti-infective pulmonary proteins: in vivo cooperative action of surfactant protein SP-A and the lung antimicrobial peptide SP-BN, J. Immunol. 195 (2015) 1628–1636.
[70] S. Singh, A. Datta, A. Schmidtchen, A. Bhunia, M. Malmsten, Tryptophan end-tagging for promoted lipopolysaccharide interactions and anti-inflammatory effects, Sci. Rep. 7 (2017) 1–14.